Int J Earth Sci (Geol Rundsch) (2014) 103:1037–1056
DOI 10.1007/s00531-014-1016-7

ORIGINAL PAPER

Partitioning of convergence in Northwest Sub-Himalaya: estimation of late Quaternary uplift and convergence rates across the Kangra reentrant, North India

V. C. Thakur · M. Joshi · D. Sahoo · N. Suresh · R. Jayangondapermal · A. Singh

Received: 1 July 2013 / Accepted: 14 March 2014 / Published online: 30 March 2014

Abstract The Kangra reentrant constitutes *a* ~ 80-km-wide zone of fold-thrust belt made of Cenozoic strata of the foreland basin in NW Sub-Himalaya. Earlier workers estimated the total long-term shortening rate of 14 ± 2 mm/year by balanced cross-section between the Main Boundary Thrust and the Himalayan Frontal Thrust. Geologically estimated rate is nearly consistent with the GPS-derived slip rate of 14 ± 1 mm/year. There are active faults developed within 4–8 km depth of the Sub-Himalayan fold-thrust belt of the reentrant. Dating the strath surfaces of the abandoned fluvial terraces and fans above the thrust faults, the uplift (bedrock incision) rates are computed. The dips of thrust faults are measured in field and from available seismic (depth) profiles. From the acquired data, late Quaternary shortening rates on the Jawalamukhi Thrust (JT), the Soan Thrust (ST) and the Himalayan Frontal Thrust (HFT) are estimated. The shortening rates on the JT are 3.5–4.2 mm/year over a period 32–30 ka. The ST yields a shortening rate of 3.0 mm/year for 29 ka. The corresponding shortening and slip rates estimated on the HFT are 6.0 and 6.9 mm/year during a period 42 ka. On the back thrust of Janauri Anticline, the shortening and slip rates are 2.0 and 2.2 mm/year, respectively, for the same period. The results constrained the shortening to be distributed largely across a 50-km-wide zone between the JT and the HFT. The emergence of surface rupture of a great and mega earthquakes recorded on the reactivated HFT implies ≥100 km width of the rupture. The ruptures of large earthquakes, like the 1905 Kangra and 2005 Kashmir, remained restricted to the hinterland. The present study indicates that the high magnitude earthquakes can occur between the locking line and the active thrusts.

Keywords Active faults · Sub-Himalaya zone · Paleoseismology · Surface ruptures · Out-of-sequence faulting

Introduction

The Himalaya orogen developed by collision between the Indian and the south Eurasian plates at ~55 Ma (LeFort 1975; Molnar 1984; Yin 2006). Large-scale crustal shortening induced by northerly drift of the Indian plate, accompanied regional thrusting that generated from N to S, the Main Central Thrust (MCT), the Main Boundary Thrust (MBT) and the Himalayan Frontal Thrust (HFT) (Fig. 1a). These thrusts are the splays of the basal decollement/detachment called the Main Himalayan Thrust (MHT) (Zhou et al. 1993; Schulte-Pelkum et al. 2005; Nabelek and HI-CLIMB Team 2009). With the southward growth of the Himalaya, the MHT progressively developed in the forelandward propagating thrust systems as the MCT–MHT, MBT–MHT and the HFT–MHT. At present, the HFT represents the surface expression of the MHT. The crustal shortening in the Himalaya is absorbed through sequential development of foreland propagating thrust system during early Miocene to Pleistocene viz. the MCT in early Miocene (18–23 Ma), the MBT in late Miocene (9–11 Ma) and the HFT in Quaternary (<2.5 Ma). An active out-of-sequence thrust faulting during Pliocene is reported at the physiographic and

Electronic supplementary material The online version of this article (doi:10.1007/s00531-014-1016-7) contains supplementary material, which is available to authorized users.

V. C. Thakur (✉) · M. Joshi · D. Sahoo · N. Suresh · R. Jayangondapermal · A. Singh
Wadia Institute Himalayan Geology, 33 GMS Road, Dehradun 248001, India
e-mail: thakurvc@wihg.res.in; thakurvc12@gmail.com

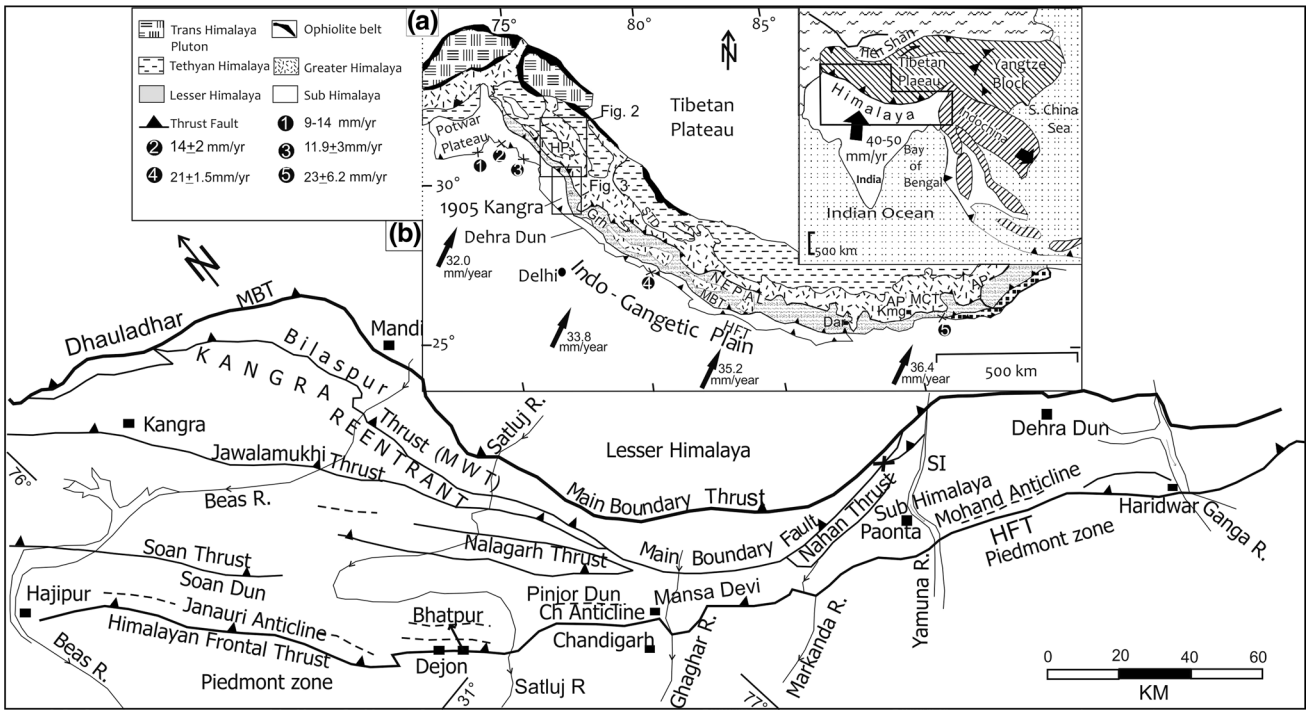

Fig. 1 **a** An outline tectonic map of Himalaya showing the principal thrusts and tectonic zones. *HFT* Himalayan Frontal Thrust, *MBT* Main Boundary Thrust, *MCT* Main Central Thrust, *STD* South Tibetan Detachment, *HP* Himachal Pradesh, *Grh* Garhwal, *Da* Darjeeling, *AP* Arunachal Pradesh, *Kmg* Kameng. *Arrows* indicate convergence rate of India with respect to Tibet. In legend, 1–5 numbers in *circle* indicate geologically estimated shortening rates. *Inset* rectangles of Figs. 2 and 3 (after Thakur 2013). **b** Outline tectonic map of Sub-Himalaya between the Beas and the Ganga rivers, showing major thrusts, frontal anticlines, duns and major locations (after Thakur et al. 2007)

thermo-chronologic boundary, south of the MCT between the Lesser Himalaya and the Higher Himalaya in central Nepal and NW Himalaya (Fig. 1a) (Wobus et al. 2006; Mukherjee et al. 2012; Mukherjee 2013). Out-of-sequence active faulting north of the HFT is observed from the Darjeeling Sub-Himalaya (Mukul et al. 2007), between the MBT and the HFT in the Dehradun region (Fig. 1b) (Thakur et al. 2007; Mukherjee 2014). 2005 Kashmir earthquake surface rupture occurred along out-of- sequence Balakot–Bagh fault (Kaneda et al. 2008; Hussain et al. 2009).

The Indian plate has been subducting below southern Eurasia at a convergence rate of 45-50 mm/year since collision. Of the total convergence, ~10–20 mm/year is accommodated in the Himalaya and rest is distributed in Tibet and southern Eurasia (Lyon-Caen and Molnar 1985; Armijo et al. 1986; Avouac and Tapponnier 1993; Peltzer and Saucier 1996). In the central sector, i.e., Nepal Himalaya, the convergence rate of 20 ± 1–3 mm/year was derived both on long-term and short time scales based on Holocene strath terraces (Lave and Avouac 2000) and GPS measurements (Bilham et al. 1997; Jouanne et al. 2004; Bettinelli et al. 2006). In NW Sub-Himalaya, the shortening rates of 11 ± 5 mm/year across the HFT were estimated on long term (Powers et al. 1998) and during late Holocene (Wesnousky et al. 1999) across Dehradun in Garhwal (Fig. 1b). In the Kangra reentrant (Fig. 1b), 14 ± 2 mm/year shortening rate was deduced from balanced cross-section (Powers et al. 1998) and 14 ± 1 mm/year slip rate on the MHT derived from GPS measurements (Banerjee and Burgmann 2002). These observations suggest that the Holocene rates of deformation can be taken as good indicator for long-term rates of elastic strain accumulation. In the Kangra reentrant and region to its north, the instrumental recorded seismicity is concentrated beneath the MCT-MBT zone over the Dhauladhar range and farther north in the Chamba sequence of Lesser Himalaya (Fig. 2). Microseismicity south to MBT in the Kangra reentrant is either absent or is sporadic (Thakur et al. 2000; Kumar et al. 2009). The Kangra reentrant was affected by the 1905 Kangra earthquake of magnitude Mw 8 (Middlemiss 1910) revaluated to 7.8 (Ambreys and Bilham 2000, Wallace et al. 2005). Our study area lies in the meizoseismal region of this earthquake. The source zone of the 1905 earthquake with respect to the seismogenic nature of the major faults in the reentrant region is not well understood (Figs. 1, 2). Quaternary-Holocene shortening-slip rates can help in understanding the dynamics of mountain building and variation in deformation across the locked segment of

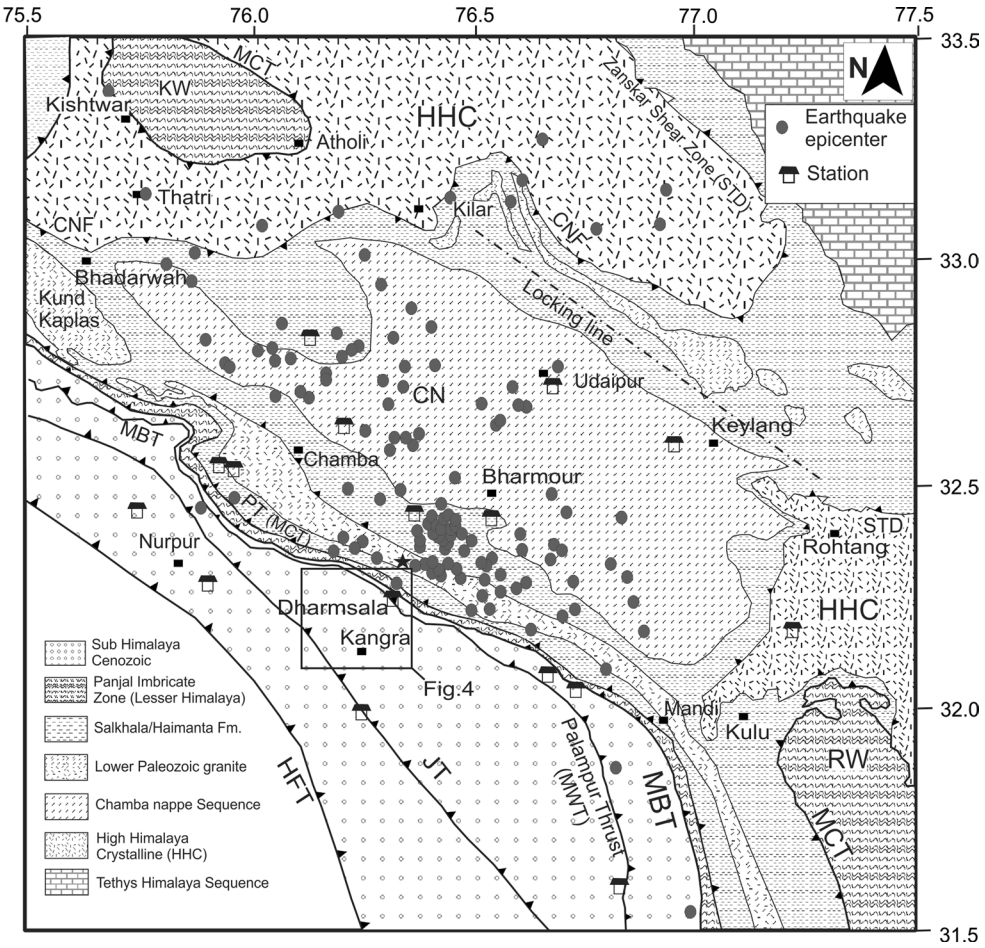

Fig. 2 Microseismicity map of Kangra reentrant, Chamba nappe sequence and adjoining areas of Higher Himalaya and window zones. *Filled circles* represent epicenters and huts are seismic stations. *Star* represents probable location of 1905 Kangra earthquake epicenter. Locking *line* lies north of the microseismicity belt. *Inset square* represents study area. *CN* Chamba Nappe, *RW* Rampur Window, *KW* Kishtwar Window, *HHC* Higher Himalaya Crystalline, *MWT* Medlicott Wadia Thrust, *JT* Jawalamukhi Thrust. (Seismicity map modified after Kumar et al. 2009, background geology after Thakur 1998)

the MHT. Estimation of Quaternary-Holocene deformation rates in the Kangra reentrant may unravel the nature and distribution of deformation rates on the major faults across the Sub-Himalaya, thereby providing a deeper insight into the seismic hazards in this region.

The Kangra reentrant in the Sub-Himalaya of Himachal Pradesh, NW India, lies between the Dhauladhar range of the Lesser Himalaya and the Indo-Gangetic plains (Figs. 1, 3a). It is a part of the Cenozoic foreland basin. A wide belt of the fold-thrust belt of the lower Tertiary and the Neogene Siwalik Group is exposed between the MBT and the HFT in the Kangra reentrant (Karunakaran and Rao 1979; Raiverman et al. 1994) (Fig. 3a, b). The HFT, the ST, the JT and the Palampur Thrust (PT) are active faults in the reentrant (Yeats et al. 1992; Wallace et al. 2005; Thakur et al. 2010). These thrust faults splay off from the basal decollement (MHT). There are well-preserved fluvial strath terraces and uplifted fan strath surfaces in the study area. Seismic profiles and bore-well data of the Oil and Natural Gas Commission (ONGC) provide subsurface dips of the thrust faults and geometry of the structures (Raiverman et al. 1994; Powers et al. 1998). The optical stimulated luminescence (OSL) dating of the sand–silt in gravel cover over the strath terraces assigns the abandonment ages of the terraces. The strath terraces have been used earlier to estimate the uplift, shortening and slip rates on the HFT in the Himalaya (Wesnousky et al. 1999; Lave and Avouac 2000). In the present investigation, uplift (incision) and shortening rates are estimated using uplifted strath terrace surfaces on the hanging walls of the JT, ST and an abandoned alluvial fan overlying the Siwalik strata on the uplifted hinge zone of the upright and symmetric Janauri anticline. The anticline lies at the hanging wall of the HFT (Fig. 3a, b).

Geology

East of the Kashmir–Hazara syntaxis, the Sub-Himalayan Cenozoic sequence of foreland basin attains a maximum width of ~80 km, between the Ravi and Satluj rivers in the Kangra reentrant (Fig. 1). The foreland basin is bounded in the north by a narrow, a few km wide, belt of the Panjal Imbricate zone of the Lesser Himalaya along the MBT. The Lesser Himalayan zone itself in turn is overlain along the Panjal Thrust (~MCT), by the Chamba nappe sequence, constituting the Dhauladhar and Pir

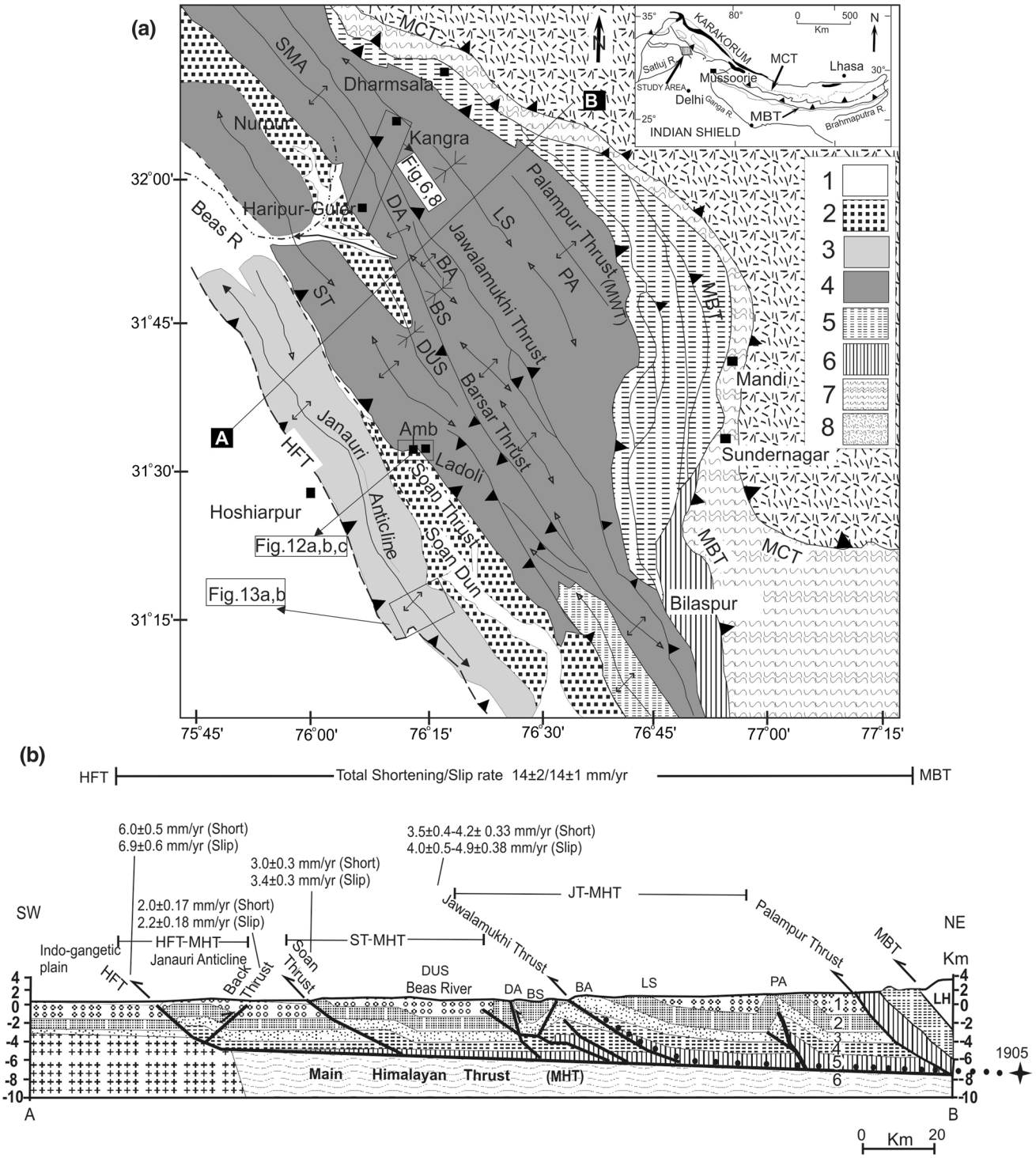

Fig. 3 **a** Regional geological map of Kangra reentrant. Inset rectangles representing Figs. 6, 8, 12a–c, 13a, b are the study areas. *MCT* Main Central Thrust, *MBT* Main Boundary Thrust, *PA* Paror Anticline, *LS* Lambagaon Syncline, *BA* Balh Anticline, *BS* Balaru Syncline, *DA* Dehra Gopipur Anticline, *DUS* Dumsa syncline, *ST* Soan Thrust, *HFT* Himalayan Frontal Thrust. *1* Alluvium, *2* Dun alluvial fan deposit, *3* Frontal Siwalik range, *4* Undifferentiated Siwalik, *5* Dharamsalas, *6* Subathus, *7* PIZ Lesser Himalaya formations, *8* High and Tethys Himalayas (Map modified after Powers et al. 1998; Delcaillau et al. 2006). **b** Balanced cross-section across Kangra reentrant based on A–B line in **a**, showing major structures, estimated shortening and slip rates on the thrust faults. *1* Upper Siwalik, *2* Middle Siwalik, *3* Lower Siwalik, *4* Upper Dharamsala, *5* Lower Dharamsala, with thin Subathu, *6* Pre-Cambrian–Cambrian metasedimentaries (Vindhyan Group), *7* Pre-Cambrian Crystalline basement, *PA* Paror Anticline, *LS* Lambagaon Syncline, *BA* Balh Anticline, *BS* Balaru Syncline, *DA* Dehra Gopipur Anticline, *DUS* Dumsa Syncline (after Powers et al. 1998)

Panjal ranges (Fig. 2) (Thakur 1998). South of the MBT, the Kangra reentrant constitutes lower Tertiary sequence of the marine Paleocene–Middle Eocene Subathu and the non-marine Late Oligocene-Early Miocene Dharamsala Formations in the northern part. In the northern part, the lower Tertiary sequence is thrust along the PT over a wide belt of the Middle Miocene–Pleistocene (Neogene) Siwalik Group that occupies the central and southern parts of the reentrant (Fig. 3a). The southern part is characterized by the Soan dun intermontane basin and frontal Janauri anticline. In northern part, the Kangra intermontane basin (dun) is developed between the Dhauladhar range and the Siwalik range over the JT (Fig. 4). South of the MBT, the Palampur/Bilaspur Thrust, earlier referred as the Main Boundary Fault by Medlicott (1864) and Wadia (1937), is now renamed as the Medlicott Wadia Thrust (MWT) (Figs. 1b, 2, 3a) that extends as an active fault strand of the MBT from Jhelum to Yamuna in NW Himalaya (Thakur et al. 2010).

South of the Palampur Thrust (MWT), the Neogene Siwalik Group is characterized into three thrust packages, based on major structural style, of the JT, the ST and the HFT (Fig. 3a, b). The JT slab shows fairly uniform 25–35°NE dip becoming nearly horizontal to the north. The slab sequence is folded into a broad open Lambagaon syncline (LS) with 80 km lateral extent and a secondary Paror anticline (PA) with 20 km lateral extent (Fig. 3a, b). The JT extends NW–SE along regional strike for more than 200 km. The ST slab shows a large broad monoclinal folding in its southern part. Its northern part, which constitutes the footwall of the JT, is made of fold-thrust system of Balh anticline (BA), Balaru syncline (BS) and Dehra Gopipur anticline (DA) (Fig. 3a, b). The HFT thrust slab constitutes the Janauri anticline ridge of frontal Siwalik range and an intermontane synformal depression of the Soan dun. The fold-thrust belt of the Kangra reentrant between the HFT and the MBT is underlain by a decollement that was imaged in seismic profile and interpreted in a balanced cross-section (Powers et al. 1998).

Dhauladhar range (D-range), bordering the northern margin of the foreland basin in the Kangra reentrant, rises abruptly to 4,800–4,000 m above mean sea-level (amsl) altitude from the 700–800 m high Siwalik ranges, constituting a mountain front for focused precipitation (Fig. 4). In the adjoining Lahaul area, the southern extent of glacial advance is recorded up to 2,800 m during last glacial cycle and last glacial maximum (LGM) (Owen et al. 1997, 2002). A similar glaciation scenario is envisaged for the D-range.

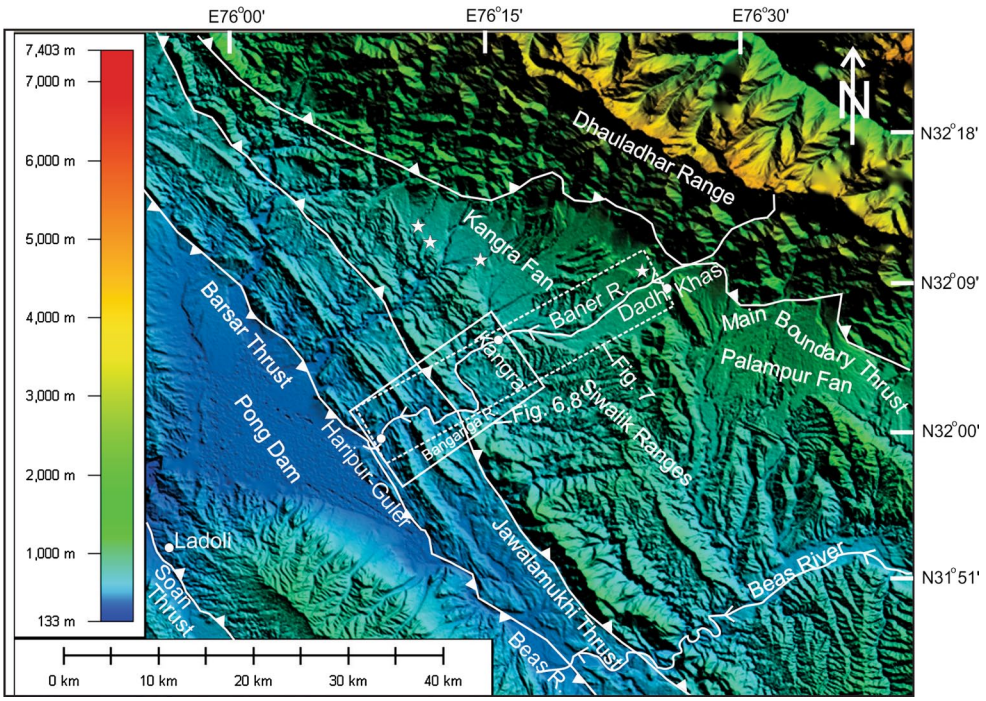

Fig. 4 SRTM image of northwestern part of Kangra reentrant and Dhauladhar range and adjoining areas. Banganga, called Baner upstream, river flowing from southern slope of the range incises the Kangra fan in northern part and the Siwalik ranges strata in southern part. *Star* indicates paleosol horizon localities, from left to right: Chambi, Gaggal airport, Yol camp golf course, and near Iku Khad Highway. The MBT, Jawalamukhi Thrust, Barsar Thrust, and Soan Thrust are demarcated. The Kangra intermontane basin, constituting the Kangra and Palampur fans, is bounded in the north by the Dhauladhar range front and the south by the Siwalik ranges. Localities: Dadh Khas, Kangra, Haripur-Guler and Ladoli. Inset rectangles: *Dash line rectangle* indicates Fig. 7 location. *Solid line rectangle* represents location of Figs. 6 and 8

Fig. 5 Debris flow, comprising unsorted large to medium size granite boulders in the proximal part of Kangra fan. *Inset photograph* showing orange-brown paleosol (pedogenised loess) horizon, ~10 m thick, occurs within the debris flow. Locality: Iku khad crossing Yol-Chamunda highway (N32°09′34.9″, E76°24′21.2″)

The Kangra basin is late Quaternary intermontane basin, ~75 km long and 10–25 km wide, bounded to the north by the D-range and to its south is framed by the Siwalik ranges. The basin was developed as a piggyback basin (Ori and Friend 1984) over the JT during late Quaternary. The Kangra intermontane basin is predominantly filled by debris flow fans produced by deglaciation in the D-range. 3–8 m thick orange-red paleosol horizons occur at several places within the fan sequence (Figs. 4, 5). Paleopedological analysis and OSL dating of paleosols revealed those as pedogenised loess (Srivastava et al. 2009). Loess deposited around ~78–44 ka in the proximal setting and ~30–20 ka in the distal setting during cold-arid conditions as glaciers advanced on the D-range. Wet–humid intervals pedogenised the loess into paleosol. Between Kangra and Guler, width of the deep-cut river channel varies 100–250 m, whereas the individual strath terrace width ranges 400–700 m. The combined channel width of Kangra T_3 or Haripur-Guler T_2 strath terraces, which occur on both sides of the river as paired terraces (Fig. 6), indicates width of

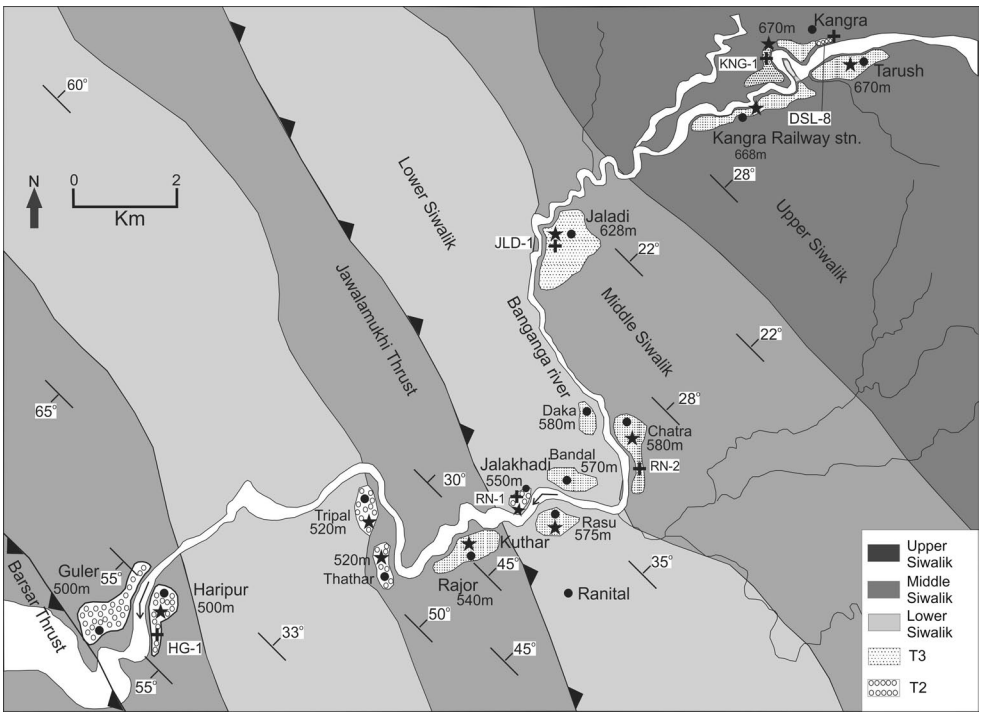

Fig. 6 Geological map between Kangra and Guler showing distribution of T_2 and T_3 strath terraces. Stippled areas represent strath terraces along the Banganga River. Dot—locality, star—altitude amsl, Cross—OSL sample locality and sample number

the channel ranging between 800 and 1,200 m. The gravel cover of the strath terraces contain (sub) rounded boulders of the Dhauladhar granite in sandy matrix. The peneplanation of wide strath terraces was by deglaciation event in the D-range. Subsequent upthrusting elevated the strath surface with gravel cover. The OSL dates, 32–30 and 17–13 ka, of the strath surfaces represent the abandonment ages of the terraces from the riverbed due to uplift.

Methodology

The fluvial strath terraces can be a proxy for estimating the tectonic uplift (Rockwell et al. 1984; Burbank et al.1996; Lave and Avouac 2000; Burbank and Anderson 2011). Assuming that the geometry and elevation of the river remain constant during downcutting, the rock uplift is equal to river incision, as measured from the elevation of abandoned strath terrace above the present-day riverbed (Lave and Avouac 2001). Using the dated fluvial strath terraces incision, the Holocene rock uplift and the shortening/slip rates on the HFT (MFT) have been estimated in the frontal part of the Sub-Himalaya near Dehradun in Garhwal (Wesnousky et al. 1999) and Central Nepal (Lave and Avouac 2000) (Fig. 1). Their estimated rates closely match the GPS determined shortening and slip rates (Bilham et al. 1997; Banerjee and Burgmann 2002). Using the paleoseismology trenches along the HFT scarps, earthquake slips have been estimated in the western Himalaya (Jayangondaperumal et al. 2013).

The present study at the Kangra reentrant distinguishes three geological settings suitable for estimating the uplift and convergence rates (Fig. 3a). From north to south, these are as follows: a) strath terraces with gravel cover on the hanging and foot walls of the JT along the Banganga, also called Baner, river section between Kangra and Guler (Fig. 4), b) peneplaned strath surface overlain by gravel and sand–silt of a remnant fan at the thrust front on the hanging wall of the ST near Amb in Soan dun (Fig. 3a), c) an uplifted flat surface with Siwalik sandstone strath surface overlain by an abandoned alluvial fan (AAF) gravel with sand–silt on the hinge zone of the southeastern part of the Janauri anticline (JA).

The geomorphic surface altitudes and vertical incised thickness above the riverbed were determined using Leica Total Station (EDM), 1:50,000 toposheets with 20-m contour interval (where line of sight for EDM not available) and ground check by hand held GPS. The OSL samples for dating were extracted from the sand–silt-rich layers and lenses in the gravel beds immediately, ~1–2 m, above the strath surfaces. The dating was done using optically stimulated luminescence (OSL) technique at the Wadia Institute of Himalayan Geology, Dehradun laboratory. The measurements were made with blue light emitting diodes (Riso TL/DA 20 reader, Riso, Denmark) and following the standard Single Aliquot Regeneration (SAR) protocol (Murray and Wintle 2000). Calibrated $^{90}Sr/^{90}Y$ beta source attached to the Riso readers artificially irradiated. The equivalent dose (ED) values were calculated by Duller's Analyst software (Dutta et al. 2012), using initial integral of the OSL. To estimate the annual dose rate, concentrations of uranium, thorium and potassium in the sediments were measured by the XRF. The water content was determined for all the samples by heating at 100 °C. The OSL ages obtained in the area are presented in Table 1. The bedrock uplift (incision) rate was determined as height (thickness) of the strath terrace above the riverbed versus the OSL age.

The Kangra reentrant region has been investigated extensively for hydrocarbon exploration by the Oil and Natural Gas Commission (ONGC) (Karunakaran and Rao 1979; Raiverman et al. 1994). Based on the ONGC data, a balanced cross-section was prepared and subsurface dips of the thrust faults indicated (Fig. 3b) (Powers et al. 1998). In our estimated of shortening and slip rates, dip of the thrust faults was deduced from the seismic profile sections combined with our field measurements. The bedrock incision of strath terraces on the hanging walls of the thrust faults was presumably attributed to uplift by shortening/slip accommodated on the faults. The JA developed as a fault-propagation fold with pop-up fold geometry (Powers et al. 1998) with a back thrust over the HFT. Anticline uplifted by HFT–MHT slip. The computation of shortening and slip rates on the JT, ST, HFT and back thrust are explained below.

The vertical component of slip of thrust planes in an upthrust movement produces uplift of the hanging wall. In a

Table 1 Giving sample number, equivalent dose, dose rate and computed optically stimulated luminescence (OSL) ages

Sample no		Equivalent dose (Gy)	Dose rate (Gy/Ka)	Age (Ka)
Lab	Field			
LD-310	KNG1	113.99 ± 12.47	3.50 ± 0.07	32.58 ± 3.62
LD-312	DSL8	89.46 ± 12.59	5.13 ± 0.07	17.44 ± 2.46
LD-916	RN-2	188.21 ± 6.80	6.12 ± 0.43	30.80 ± 2.40
LD-915	RN-1	86.37 ± 10.34	3.78 ± 0.26	22.8 ± 3.16
LD-917	HG-1	69.33 ± 6.16	5.32 ± 0.32	13.00 ± 1.40
LD-358	L2	133.80 ± 11.80	4.60 ± 0.06	29.00 ± 2.60
LD-197	JA	169.13 ± 7.49	3.93 ± 0.27	42.94 ± 3.57
LD-198	KT-1	93.76 ± 26.28	3.77 ± 0.26	24.89 ± 7.18
LD-199	KT-2	48.39 ± 7.67	3.98 ± 0.26	12.17 ± 2.09
LD-200	IS-1	91.48 ± 0.91	3.86 ± 0.39	23.70 ± 5.50
LD-201	IS-2	66.23 ± 0.66	3.78 ± 0.38	17.53 ± 4.90
LD-624	SD-2	48.53 ± 1.2	4.9 ± 0.05	12.0 ± 2.60

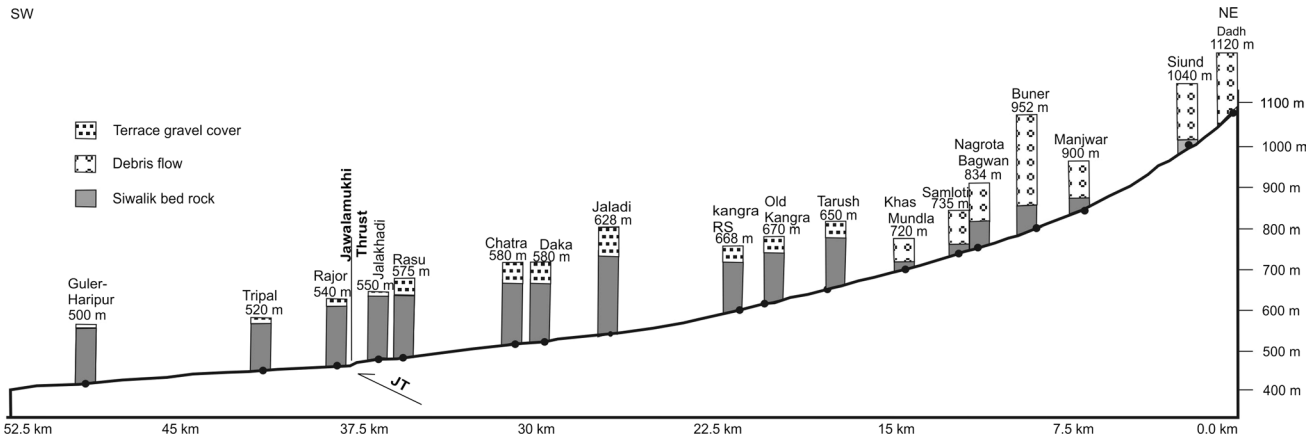

Fig. 7 Riverbed profile of Baner (Banganga) River between Dadh Khas in the Kangra fan proximal part and Guler-Haripur in the distal part of strath terraces (NE–SW), showing incision thickness of strath (Siwalik bedrock), and debris flow of Kangra fan and gravel cover of strath terraces above the riverbed surface profile. The altitudes amsl of localities are indicated above the logs. Thickness of bedrock strath increases form NE to SW, whereas thickness of debris flow-gravel cover decreases NE–SW. Vertical scale in profile section shows altitude amsl with respect to river profile. *Vertical scale* of the logs is enlarged two times above the riverbed for better representation

strath terrace, surface overlying the hanging wall of a thrust fault: (i) dip of the fault (α) and, (ii) vertical displacement deduced from the height of the strath scrap (Vi = incised bed rock thickness) above the riverbed or fan surface are determined. Having these values, shortening and slip rates are estimated using the Eqs. (1) and (2) (modified after Jayangondaperumal et al. 2013) (Supplementary Fig.S1-a, b, c).

$$\text{Shortening} = \text{Vi}/\tan\alpha \quad (1)$$

$$\text{Slip} = \text{Vi}/\sin\alpha \quad (2)$$

The shortening and slip rates of JT and ST are estimated using (a) dip of HFT (α) deduced form seismic profile and balanced cross-section (Powers et al. 1998) and our field observation, and (b) Vi = vertical thickness of strath terrace or fan surface above riverbed. In the fault-propagating pop-up JA, height (h) of strath surface at the anticline hinge zone (HZ) is determined with respect to Panjab alluvial plain (Pap) between strath surface hinge zone (HZ) line and Panjab alluvial plain (Pap) line. An inverted right angle triangle is constructed between Pap line and HZ line by drawing a perpendicular at intersection between HFT and termination of foreland limb against Pap line (Supplementary Fig. S1-d). Having determined (i) height (h) of the hinge zone strath surface with respect to Panjab plain and, (ii) dip of the HFT; shortening and slip rates were estimated on the HFT using the Eqs. (3) and (4). The same Eqs. (3, 4) are applied in estimating the shortening and slip rates for the back thrust (Supplementary Fig. S1-d).

$$\text{Shortening} = h/\tan\alpha \quad (3)$$

$$\text{Slip} = h/\sin\alpha \quad (4)$$

Uplift rates using the Banganga strath terraces

The Banganga (Baner) River in its upper reaches north of Kangra, flows SW from the southern slope of the D-range and drains into the Pong dam reservoir erected across the Beas River (Fig. 4). The river incises the Kangra fan sediments of the Kangra intermontane basin in the northern part, and the Siwalik group strata of the Siwalik ranges in the southern part produce two to three levels of valley fill in the former case and strath terraces in the latter case (Figs. 4, 7). The Kangra alluvial fans dip S, and SW flowing streams cut them. Gravely facies debris flows dominate the Kangra fan in its proximal part, and subordinate fluvial deposits in the middle and distal part. North of Kangra at altitude between 1,120 and 720 m, the Banganga River incises the Kangra fan, exposing ~100-m-thick fluvial to glacio-fluvial deposit with a few meters thick underlying bedrock exposed in the proximal part. In the middle to distal part of the fan, the river incision shows thinning fan cover sediments with thickening of underlying Siwalik strath. Whereas south of Kangra between Kangra and Guler at altitude between 670 and 500 m in the Siwalik range, the river incises 40–88 m of Siwalik strath with 5–20-m-thick fluvial gravel cover (Fig. 7). These observations suggest that bedrock incision of the strath terraces in the Siwalik strata observed south of Kangra primarily occurred due to bedrock uplift. The uplift of the strath terraces is attributed to the activation of JT.

We mapped the strath terraces along the Banganga River between Kangra and Guler (Fig. 6). There are several levels of abandoned river terraces. However, we focused on the two prominent levels of strath terraces (T_2 and T_3) with gravel cover. The T_2 and T_3 terraces show well-developed

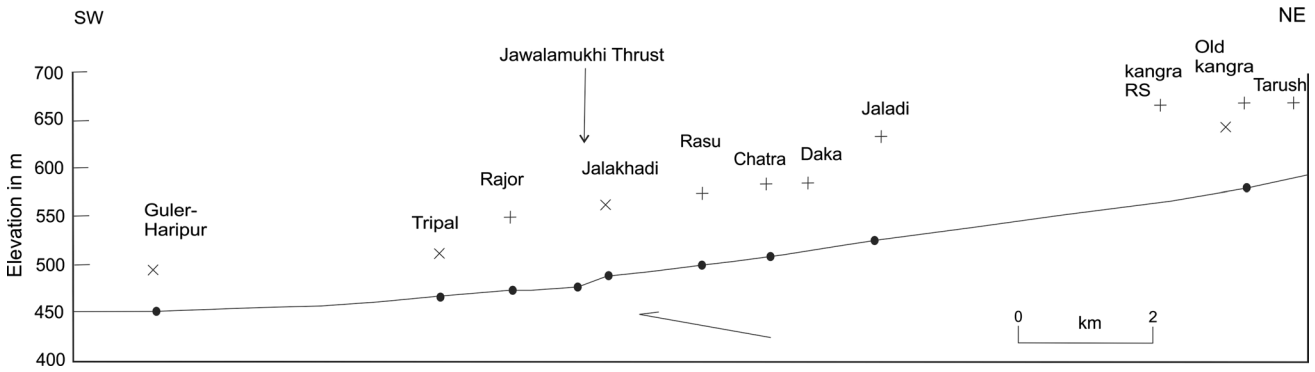

Fig. 8 Longitudinal surface gradient profile of the riverbed along the Banganga River between Kangra and Guler. Dot on the profile denotes location of the terraces. Plus indicates surface location of the T_3 terrace, and cross indicates surface location of the T_2 terrace with respect to altitude amsl. A knickpoint between the Rajor and Jalakhadi localities corresponds to the Jawalamukhi Thrust trace

vast peneplains. South of the Kangra town suburb, two well-preserved levels of strath terraces (T_2 and T_3) are observed on the Banganga River at Kangra bypass, Tarush and Kangra railway station (Fig. 6). The Chatra terrace on the left bank is similar in age, 30 ka, to that of the Kangra T_3 terrace. The Jalakhadi terrace yields 23 ka age, closer to the Kangra terrace T_2 than the T_3 terraces. The Daka and Bandal are paired to Chatra and Rasu and hence are grouped under T_3 terraces (Fig. 6). The Rajor on the footwall has similar peneplane with size and gravel cover to that of the T_3 terraces on the hanging wall. It is therefore classified under T_3 terraces. The Haripur and Guler are paired terraces and younger in age of 13 ka than the T_3 of 30–32 ka and hence classified as the T_2. The Thathar and Tripal terraces have peneplains with size and gravel cover resembling to that of the T_2 Haripur and Guler. (Fig. 6). The OSL dating was undertaken in five terraces, namely the Kangra T_3, Kangra T_2, Chatra T_3, Jalakhadi T_2 and Haripur T_2 (Table 1).

A NE-SW longitudinal profile was constructed along the riverbed of the Banganga River between Kangra and Guler (Fig. 8). The incised vertical thickness of the strath terraces above the riverbed was measured by placing the total station on the riverbed and line of sight prism placed at the terrace top. The gravel thickness was measured on the outcrop. This procedure was followed for all the terraces, except Chatra and Jalakhadi where suitable locations for line of sight prism were not found. Therefore, topographic 20-m contours (1:50,000 scale Survey of India toposheet) and GPS were used. The riverbed surface gradient profile, NE-SW, along the river between Guler and Kangra was constructed. The riverbed altitude was determined using 20-m contour at localities where the contour line intersects the riverbed in the Survey of India topographic map. The altitudes amsl of terrace top surfaces are projected above the riverbed profile. There is a break in the slope of riverbed gradient surface characterized by a knickpoint between Rajor and Jalakhadi (Fig. 8). The break closely corresponds

Table 2 Giving vertical incision/uplift, age; and uplift, shortening and slip rates

Terrace	Vertical incision (m)	Age (ka)	Uplift (mm/year)	Shortening (mm/year)	Slip (mm/year)
Jawalamukhi thrust					
Kangra T3 (KNG1)	65	32.6 ± 3.6	2.0 ± 0.22	3.5 ± 0.39	4.0 ± 0.5
Kangra T2 (DSL8)	49	17.4 ± 2.4	2.8 ± 0.39	4.9 ± 0.68	5.6 ± 0.77
Chatra T3(RN2)	75	30.8 ± 2.4	2.4 ± 0.19	4.2 ± 0.33	4.9 ± 0.38
Jalakhadi T2 (RN1)	75	22.8 ± 3.2	3.3 ± 0.46	5.7 ± 0.8	6.6 ± 0.93
Haripur-Guler T2 (HG 1)	40	13.0 ± 1.4	3.1 ± 0.33	5.3 ± 0.57	6.2 ± 0.67
Soan thrust					
Ladoli strath (L2)	50	29.0 ± 2.6	1.7 ± 0.15	3.0 ± 0.27	3.4 ± 0.31
Himalayan frontal thrust					
Vertical uplift					
Strath surface on JA hinge zone	150	42.9 ± 3.5	3.4 ± 0.28	6.0 ± 0.49	6.9 ± 0.56
Back thrust					
	70	42.9 ± 3.5	1.6 ± 0.12	2.0 ± 0.17	2.2 ± 0.18

to the trace of the JT. The southern margin of the JT is characterized by a physiographic break observed in the SRTM and Google images and topographic map. The physiographic break nearly coincides the trace of the JT. Four terraces are studied along the Banganga River for estimating the uplift and shortening rates. Estimate of uplift rate assumed (i) the incision of the strath terrace represents the bed rock uplift and (ii) the hanging wall block JT uplifted by slip. The estimated uplift rate value represents a minimum, as there may be a minor role of climate in incision (Table 2). The uplift (incision) rates estimated for the four strath terraces are given below.

(a) Kangra Terraces (N32°05′48.6″, E76°16′6.9″): Three levels of strath terraces, T_1, T_2 and T_3, are observed along the Banganga River south of Kangra town (Figs. 6, 9a). The terrace T_1 represents an abandoned river bank. It comprises 7-m-thick Siwalik sandstone overlain by 7-m-thick gravel. The Siwalik sandstone dips 30°NE, and the gravel consists of boulders and pebbles of granite and quartzite within sand–silt matrix. The straths T_2 and T_3 represent surfaces of the incised (uplifted) Siwalik sandstone dipping 30°NE. The terrace T_2 strath surface occupies a lower level than T_3 on the abandoned left bank, whereas the same surface on the right bank is 49 m elevated above the riverbed. It is overlain by 16-m-thick fluvial gravel. A sand layer near the base of the gravel bed gives OSL age 17.4 ± 2.4 ka. (Table 1, DSL8). The terrace T_3 strath surface at Kangra bypass on the right bank, lying at 65 m elevation above the riverbed with bed rock, is overlain by 21-m-thick fluvial gravel bed. The sand-rich horizon at the base of the gravel bed yields an OSL age 32.6 ± 3.6 ka (Table 1, KNG1). The bedrock incision (uplift) rate is calculated based on strath surface elevation from riverbed versus OSL age. The bedrock incision (uplift) rates for the T_2 and T_3 strath surfaces are 2.8 ± 0.39 mm/year and 2.0 ± 0.22 mm/year, respectively.

(b) Chatra Terrace (N32°01′57.3″, E76°14′49.3″): The Chatra terrace, T_3, lies at an altitude of 580 m amsl on the left bank. The strath terrace is made of middle Siwalik sandstone dipping 28° NE. The terrace strath surface is at 75-m elevation above the riverbed (Figs. 6, 9a). It is overlain by 5-m-thick gravel bed. The gravel consists of subrounded boulders and pebbles of granite, quartzite and sandstone. A sand layer in the gravel provides a sample (Table 1, RN2) for the OSL dating. The sample is taken 2 m above the contact between the Siwalik sandstone strath surface and the overlying gravel. The OSL dating gives an age 30.8 ± 2.4 ka. The uplift (incision) rate calculated for the Chatra terrace is 2.4 ± 0.19 mm/year.

(c) Jalakhadi terrace (N32°01′15.1″, E76°13′25.7″): The Jalakhadi terrace, T_2, is exposed at an altitude of 550 m amsl on the right bank of the river (Figs. 6, 9b). Its strath surface is at 75-m elevation above the riverbed, and this surface is overlain by 5-m-thick gravel. The gravel consists of boulders and pebbles of granite, sandstone and quartzite in sand matrix. An OSL sample (Table 1, RN1) obtained from the sand layer in the gravel bed, 2 m above the strath surface, yields an OSL of age 22.8 ± 3.2 ka. The uplift (incision) rate for the Jalakhadi terrace is 3.30 ± 0.46 mm/year.

d) Haripur and Guler (N32°00′12.7″, E76°09′11.5″) terraces: The Haripur and Guler are T_2 paired terraces at an altitude of 500 m amsl along the river (Figs. 6, 9b). These terraces lying 40 m above the riverbed consists of Siwalik sandstone dipping 30°NE overlain by 5-m-thick gravel. The gravel consists of boulders and pebbles of quartzite, sandstone and granite in sandy matrix. The sand near the gravel base, 1 m, overlying the Haripur strath surface gives an OSL age of 13.0 ± 1.4 ka (Table 1, HG1). The uplift (incision) rate calculated for the Haripur terrace is 3.1 ± 0.33 mm/year.

Fig. 9 **a** *1* Kangra terraces: Three levels of strath terraces: T_1 (7 m), T_2 (49 m), T_3 (65 m) above riverbed, overlain by gravel cover 7–21 m thick. T_0 is the present-day riverbed. Locality south of Kangra, near Kangra bypass. Star-sample number and OSL age. Lithologies: clast supported gravel overlain by 8-m-thick sand–silt in T_2, and sand–silt interbedded between clast supported gravel in T_3. Field photograph below showing T_1, T_2, T_3 strath terraces above the Banganga riverbed indicated by white arrows. Photograph above is a typical T_2 strath terrace: gravel cover above white line, and Siwalik sandstone below white line. *2* Chatra terrace: Strath terrace surface 75 m above the riverbed, overlain by gravel 5-m-thick cover. Star-locality with sample number and OSL age. Lithologies: Clast supported gravel with thin sand horizon. Photograph below showing T_3 terrace with respect to Banganga riverbed seen on SE corner of the photograph. Strath terrace T_3 trace is indicated by white arrows. *Inset rectangle* shows closer view of the sample locality. Figure 9b. *3* Jalakhadi terrace: Strath terrace surface 75 m above the riverbed, overlain by gravel cover 5 m thick. Star-locality with sample number and OSL age. Lithologies: Clast supported gravel with sand lenses at the base. *Photograph above* shows trace of Jalakhadi strath surface above the riverbed, and inset photograph with closer enlarged view of sample locality. *Photograph below* shows Rajor strath surface 70 m above the riverbed (*white arrows* indicate strath terrace surface). *4* Haripur terrace: Strath terrace surface 40 m above the riverbed, overlain by 5-m-thick gravel cover. Guler terrace is paired on the right bank of the river. Star-locality with sample number and OSL age. Lithologies: Clast supported gravel with sand lenses at the base. Photograph above with *black arrows* indicates trace of the Guler strath terrace, and photograph below with *white arrows* shows trace of the Haripur strath terrace above the riverbed

Convergence rate on the Jawalamukhi Thrust

The JT is NW–SE trending major structure (>200 km) sub-parallel to the regional strike thrusting the Lower Siwalik strata over the middle and upper Siwaliks (Karunakaran and Rao 1979; Raiverman et al. 1994; Powers et al. 1998). It marks a physiographic break at the

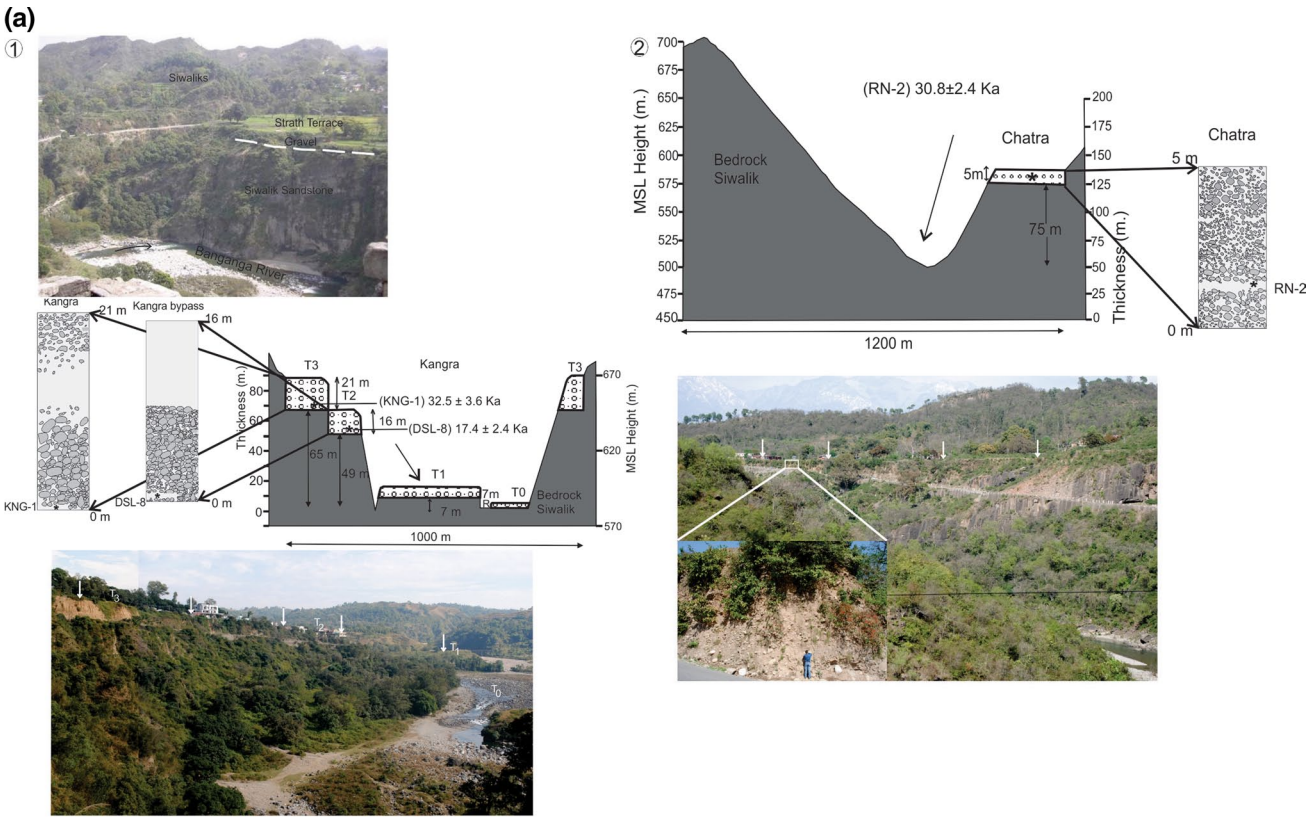
(a)
①
Siwaliks
Strath Terrace
Gravel
Siwalik Sandstone
Banganga River
Kangra
21 m
Kangra bypass
16 m
T3
T2
T1
T0
21 m
(KNG-1) 32.5 ± 3.6 Ka
16 m
(DSL-8) 17.4 ± 2.4 Ka
65 m
49 m
7m
7 m
Bedrock
Siwalik
KNG-1
DSL-8
0 m
1000 m
Thickness (m.)
MSL Height (m.)
②
(RN-2) 30.8±2.4 Ka
Bedrock
Siwalik
Chatra
5m
75 m
5 m
RN-2
1200 m
MSL Height (m.)
Thickness (m.)
(b)
③
④
Jalakhadi
5 m
(RN-1) 22.8± 3.2Ka
5 m
Rajor
5m
75 m
70 m
Bedrock
Siwalik
RN-1
Guler
5 m
(HG-1) 13.0±1.4 Ka
Haripur
5m
40 m
HG-1
1500m

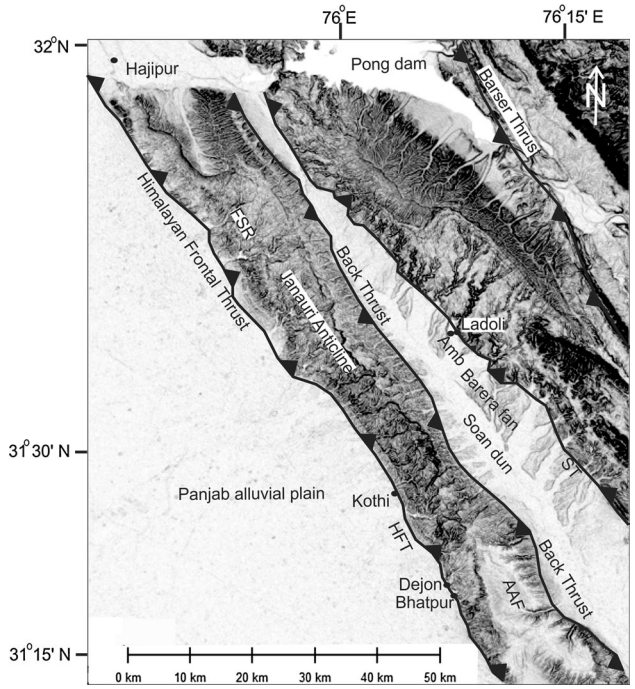

Fig. 10 SRTM image showing tectonic framework of Janauri Anticline ridge and Soan Dun. *HFT* Himalayan Frontal Thrust, Barsar thrust, *ST* Soan Thrust, *FSR* frontal Siwalik range, *AAF* Abandoned Alluvial Fan on the flat top hinge zone of the Janauri anticline (*light shade*). Localities Amb, Kothi, Dejon, Hajipur and Bharatpur mentioned in the text are shown

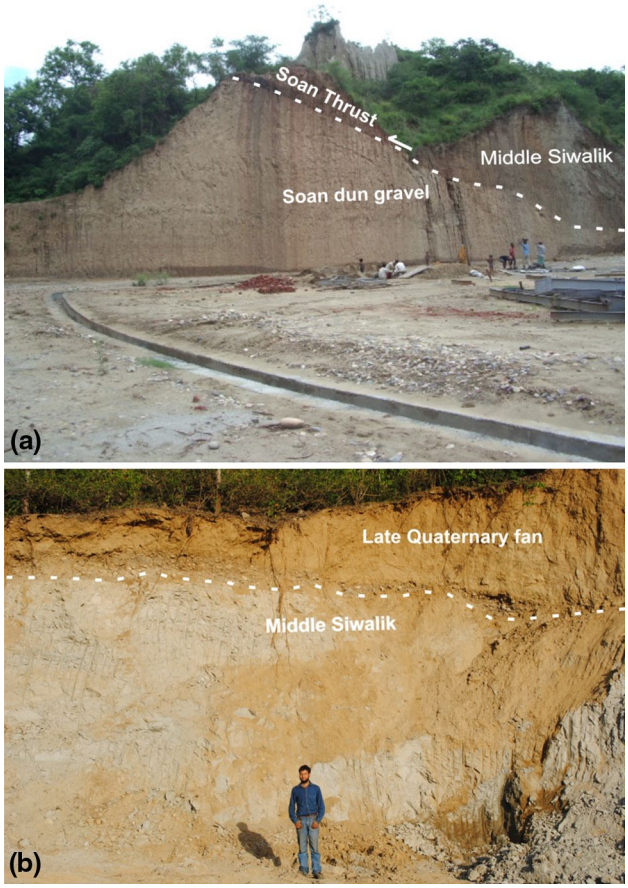

Fig. 11 **a** Middle Siwalik sandstone overriding the Amb fan sediment of the Soan dun along Soan Thrust (shown in *dotted line*). The Soan dun sediment has yielded OSL ages ranging 20–10 ka. Locality near Amb (after Suresh and Kumar 2009). **b** Middle Siwalik sandstone strath overlain by sand–silt cover of late Quaternary fan, near Ladoli

base of the southern margin of the Jawalamukhi mountains (Fig. 4). The thrust imaged in seismic profile showed a mean 30°NE dip. The T_3 terraces having the similar ages (30–32 ka) (Table 2) but occupying different altitudes (Figs. 6, 8) suggest that the terraces deformed by fold developed over the JT. The T_3 and T_2 terraces on the hanging wall are at higher altitudes than those on the footwall, indicating that the terraces are displaced by the JT (Fig. 8). The strath terraces, lying over the hanging wall of the JT, were uplifted as a result of slip (displacement) on the thrust fault. The riverbed surface gradient profile (Fig. 8) show a gentle slope with a break, knick point, which nearly corresponds to location of the JT trace. In the field, trace of the JT lies north of Rajor at the base of the southern front of the Jawalamukhi range.

In central Nepal, the Holocene convergence rate at 21 ± 1.5 mm/year on the MFT (HFT) is determined using strath terraces over the hanging wall of the fault with a fault-bend fold in the Siwaliks (Lave and Avouac 2000). The shortening/slip rate of 13 mm/year is also estimated on the HFT using an uplifted strath surface at the Siwalik front scarp on the hanging wall of the HFT, south of Dehradun in Garhwal (Wesnousky et al. 1999). These rates are found to be nearly equal to the values determined by GPS geodetic measurements (Bilham et al. 1997; Banerjee and Burgmann 2002). Both these determinations suggest that the uplift and convergence/slip rates calculated through fluvial strath terraces on the hanging walls give fairly good estimates. In the Kangra reentrant, the Siwaliks bedrock incision rates calculated for the Kangra, Chatra and Jalakhadi terraces are considered as the uplift rates (Table 2). Having determined the bedrock uplift rate and the 30°NE dip for JT from seismic profile and field observation, the convergence (shortening) and slip rates on the JT are calculated (Table 2). The shortening rates derived from the Kangra T_3 and Chatra T_3 terraces are 3.5 ± 0.39 mm/year and 4.2 ± 0.33 mm/year over the period 32.6 ± 3.6 and 30.8 ± 2.4 ka, respectively. The shortening rate computed from the Kangra T_2 terrace is 4.9 ± 0.68 mm/year for 17.4 ± 2.4 ka and for the Haripur T_2 terrace is 5.3 ± 0.57 mm/year over a period 13.0 ± 1.4 ka. The mean shortening rate estimated from T_2 and T_3 terraces is 4.45 ± 0.49 mm/year. Similarly the slip rates calculated from the terraces are indicated in Table 2.

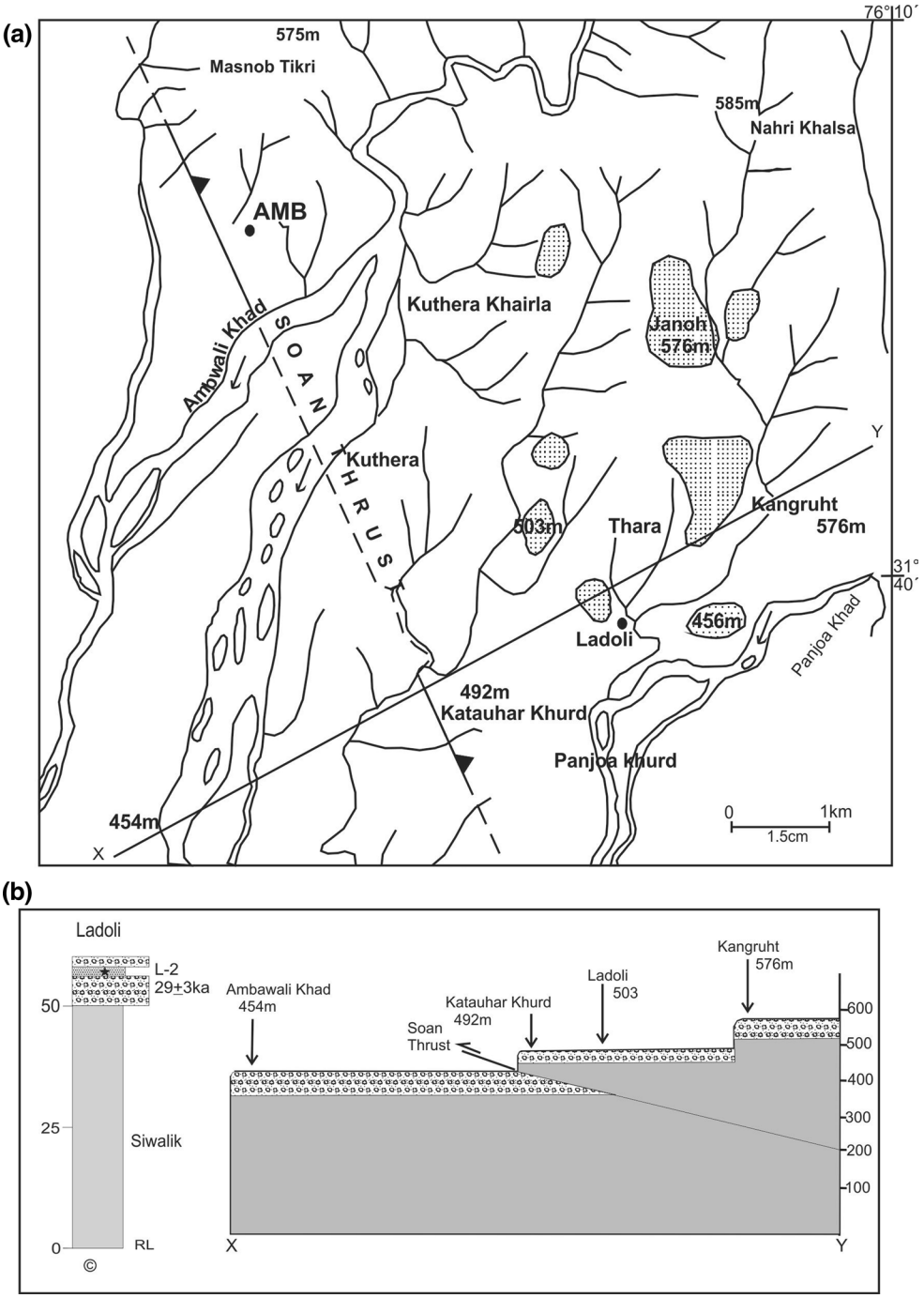

Fig. 12 **a** Location and geological setting of the locality Ladoli studied near Amb in Soan dun. Stippled area represents gravel and silt–sand cover sediment overlying the peneplaned Siwalik strata. Altitude amsl of localities indicated in m after Survey of India toposheet with scale 1:50,000. **b** Cross-section, XY, across Soan Thrust, showing location of Ladoli and two levels of surfaces. **c** Lithology column constructed from the exposed scarp showing the OSL sample location and corresponding age

Uplift and convergence rates on the Soan Thrust

The Soan dun and the JA constitute the southern part of the Sub-Himalaya in the Kangra reentrant (Figs. 3a, b, 10). The Soan dun is an intermontane basin filled by post-Siwalik alluvial fan sediments. It is bounded to the north by the raised hinterland Siwaliks and to the south by the JA of the frontal Siwalik range. Along the northern margin of the Soan dun, the ST marks a tectonic and physiographic boundary between the Middle Siwalik sandstone or the Upper Siwalik conglomerate of the hinterland Siwaliks and the late Quaternary-Holocene Soan dun sediments. On the northwestern part of the Soan dun, the raised Siwaliks abut against the flat lying Soan dun sediments along the ST (Fig. 10). At a locality near Amb, the Middle Siwalik sandstone overrides the gravel and sand–silt sediments of the Soan dun Amb fan along the ST, indicating active nature of faulting (Fig. 11a). The Amb fan sediments have given OSL ages ranging 23–10 ka (Suresh and Kumar 2009). The Siwalik sandstone strath surface at a locality Ladoli

(Fig. 10), lying on the hanging wall of the ST, is used to estimate the uplift rate on the ST.

Near Amb in northwestern part of the Soan dun, there are isolated relatively flat areas with sand–silt and gravel cover overlying the peneplaned Siwalik strath surface (Fig. 11a, b). They form the uplifted topography of the Siwalik. The gravel and sand–silt cover overlying the Siwalik strath surface represents remnants of the fan surface that is correlated with the Amb fan prior to their uplift, but now occurring on the hanging wall area of the ST. The Siwalik strath surface with its fan cover on the hanging wall uplifted due to convergence induced displacement on the ST. The gullies and streams dissecting the Siwalik topography have exposed sections showing incision of the bed rock and strath surfaces. Near a locality Ladoli, there are two levels of peneplaned strath surface of Siwalik sandstone overlain by 5–10-m-thick silt–sand with pebble bed (Fig. 12a, b). The upper level strath lies at an altitude ~576 m amsl, and the lower level strath occurs at an altitude ~503 m amsl. At Ladoli, an incised scarp is exposed with of middle Siwalik sandstone 50-m-thick overlain by a 10-m-thick pebble and silt–sand bed (Fig. 12c). The 50-m incision thickness represents elevation difference between the Ladoli strath surface on the hanging wall and the Amb fan surface on the footwall. The sample (L-2) for OSL dating was extracted from near the base of the silt horizon overlying the Siwalik sandstone. The luminescence dating of the sample gives an OSL age 29 $\pm$ 2.6 ka. Taking 50-m incision thickness as uplift, the estimated uplift (incision) rate is 1.7 $\pm$ 0.15 mm/year for the strath surface. The 30°NE dip of the ST is deduced from the measurement of surface dip of beds near the ST and the ST imaged in the seismic profile (Powers et al. 1998). Assuming that the strath surface was uplifted as a result of shortening induced slip on the ST and knowing 30°NE dip of the fault, the estimated convergence and slip rates on the ST are 3.0 $\pm$ 0.27 and 3.4 $\pm$ 0.31 mm/year, respectively, over a period 29 ka.

Janauri anticline

Himalayan range front between the Beas and the Ganga rivers in NW Himalaya is characterized by large anticlines: Janauri, Chandigarh and Mohand (Karunakaran and Rao 1979; Raiverman et al. 1994) (Fig. 1b). These anticlines developed over the HFT as fault-propagation or fault-bent folds (Suppe 1983; Powers et al. 1998; Wesnousky et al. 1999). The Janauri anticline (JA) is SE propagating active fold structure (Delcaillau et al. 2006; Thakur 2013) constituting a ridge topography of the folded Siwalik strata. Its southern margin is demarcated against the Panjab alluvial plain by the HFT, which emerges at the surface at some places or may remain blind. The JA is developed as a fault-propagation fold over the HFT (Powers et al. 1998) (Fig. 3b). A more recent study advocates that the JA is developed as a result of fault-related growth into segments with lateral propagation leading to a single large segment through linkage of smaller segments (Malik et al. 2010a). Soan dun, an intermontane basin, lies on the backlimb of the JA that is interpreted as a piggyback basin formed at the back of an active thrust (Ori and Friend 1984; Thakur et al. 2007) (Figs. 3a, b, 10). It is filled by the post-Siwalik dun sediments deposited largely by alluvial fans originating from the mountain front of the hinterland Siwalik. The fan sediments are dated, giving optically stimulated luminescence (OSL) ages ranging 36–10 ka (Suresh and Kumar 2009). The anticline has been extensively studied including seismic profiling and drilling of three wells for hydrocarbon exploration showing the subsurface structures (Karunakaran and Rao 1979; Raiverman et al. 1994; Powers et al. 1998). The JA, trending NW–SE, forms a ~100-km-long and 12–18-km-wide anticline ridge. The ridge lies between the Beas and the Soan rivers and is divided into segments along the transfer faults.

On the southeastern segment of the JA (Figs. 3a, 13a, b), the Middle Siwalik micaceous sandstone strata dip 25–35°SW on the southern forelimb. The strata become horizontal–subhorizontal on the broad hinge zone. Further north on the backlimb, the sandstone overlain by a boulder conglomerate of the Upper Siwalik dips 30–20°NE. The fold axial trace trends NW–SE and lies south of the drainage divide of the ridge. The southern limb of the JA forms a 100–150 m high modified scarp whose base is demarcated by the HFT. On the northern limb, the Soan dun sediment abuts against the NE dipping Siwalik strata with north facing 10-m high scarp at Ispur, demarcating a south-dipping thrust fault (Fig. 13b). The thrust fault represents an imbricate of the south-dipping back thrust of earlier workers (Powers et al. 1998; Malik et al. 2010a, b). In the study area, the anticline is symmetric and upright broad open fold with flat hinge zone with both limbs dipping gently in opposite direction. There is a distinctive plateau-like feature made of a flat topped area ~10 $\times$ 5 sq km on the hinge zone of the anticline (Fig. 13a, b). Here, the upper Siwalik dipping NE gentle to sub-horizontal is overlain by the fluvial deposit which resembles the post-Siwalik Soan dun sediments. The fluvial deposit consists of unconsolidated and horizontal stratified sand, mud and gravel. There are two interpretations on the origin of the gravel deposits on the flat topped topographic surface in the central part of the anticline: (a) It is interpreted as a linked up segment developed through the linkage of two smaller segments and represents the paleo-water gap of the Satluj River (Malik and Mohanty 2006; Malik et al. 2010a). The post-Siwalik sediments are interpreted as laid down by the paleo-Satluj River which later diverted into its present course. (b)

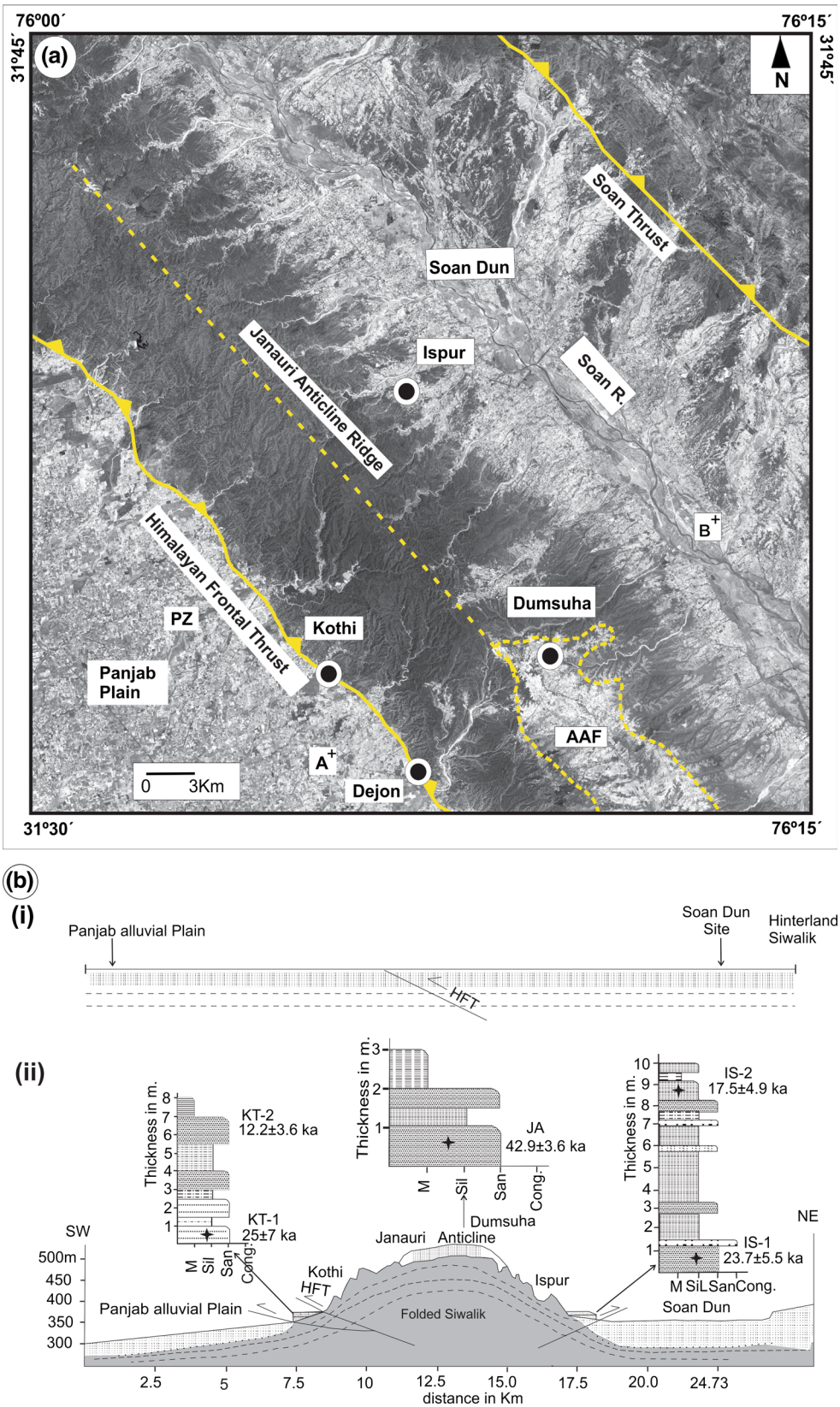

Fig. 13 **a** Satellite imagery of Janauri Anticline ridge, Soan dun and surrounding areas. Kothi on southern limb, Ispur on northern limb and Dumsuha on the hinge zone plateau: localities for OSL dating samples. AAF—Northwestern part of the Abandoned Alluvial Fan in light shade. *Dash* represents water divide on the Janauri anticline. **b** *i* Pre folding: *Broken lines* Siwalik bedrock, Mesh pattern-Post-Siwalik sediment. *ii* Post folding: SW–NE cross-section across the Janauri Anticline. *Light gray shade* with *broken lines* folded Siwalik strata. *Light gray mesh pattern* on the *hinge zone* post—Siwalik old sediment (i.e., pre growth strata). *Light gray* mesh pattern on the limbs at Kothi and Ispur: post-Siwalik horizontal bedded sand–silt represents growth strata. Lithology columns with OSL ages on the hinge zone (Dumsuha) and limbs (Kothi and Ispur)

Delcaillau et al. (2006) have described remnants of several abandoned drainage channels and weathered fluvial deposits preserved on planar interfluves in the central part of the JA and on the internal backlimb of frontal anticline. The alluvial fan deposits indicate transverse paleo-rivers intersecting the anticline ridge. The presence of elevated fans and terrace deposits developed on the planar interfluves rising up to 150 m above the alluvial plain indicate that the paleodrainage pattern is antecedent to the anticline formation. The post-Siwalik sediments, correlatable to the Soan dun fans, on the flat central part of the anticline ridge top represent the abandoned alluvial fan (AAF) (Delcaillau et al. 2006). The AAF is observed in Google Earth/SRTM image showing light shade relative to surrounding dark tone on the southeastern segment of the central part of JA ridge (Figs. 10, 13a). Traverses across the JA ridge show the AAF is >5 km wide with relatively flat topography occupying the hinge zone and water divide. The drainage on JA ridge flanks flow in NE and SW directions. The AAF is made of post-Siwalik fluvial sediments consisting of unconsolidated and horizontal stratified sand, silt, mud and gravel overlying the subhorizontal upper Siwalik strata. The post-Siwalik sediment is aggraded prior to the uplift of the anticline, an inference similar to that derived by Delcaillau et al. (2006). The sand lense from the base of the AAF sequence, overlying the Siwalik sandstone, gives an OSL age 42.9 ± 3.6 ka (Fig. 13b, Table 1, JA). In eastern Soan dun, the Barera fan (Fig. 10) sequence lying north of the AAF gives an OSL age of 36 ± 5 ka at its basal part and 29 ± 3 ka toward the top part (Suresh and Kumar 2009). The abandoned alluvial fan, AAF and the Barera fan sediments having similar lithology and about nearly the same age at the base of the sequence support Delcaillau's interpretation that the AAF represents remnant of an uplifted fan cover on the southeastward propagating anticline ridge.

The post-Siwalik sediments, comprising horizontal and stratified sand–silt–mud, also occur on the basal parts of the forelimb and backlimb of the JA at Kothi and Ispur, respectively (Fig. 13a, b). At Kothi, northwest of Dejon (Fig. 13a), on the southern limb of the anticline, the thickly bedded Siwalik sandstone dipping 30°SW abuts against the horizontal bedded post-Siwalik sediment. The post-Siwalik sediment forms a S—facing 8-m high scarp against the Panjab alluvial plain. The scarp represents emergence of HFT imbricate (Fig. 13b). The post-Siwalik sediment consists of unconsolidated, horizontal and stratified micaceous sand, silt and mud (Fig. 13b). The samples extracted from both the base and 1 m below the top at Kothi section yield OSL ages 24.9 ± 7.1 and 12.2 ± 2.0 ka, respectively (Table 1, KT1 and KT2). At Ispur on the northern limb of the anticline, the horizontally bedded post-Siwalik sediment over the 30°NE dipping Siwalik sandstone forms a north facing 10 m scarp. The base of the scarp demarcates an emergent imbricate of the back thrust (Fig. 13b). The post-Siwalik sediment consists of unconsolidated and horizontally stratified 10-m-thick micaceous sand, silt, clay and mud. The samples are taken from the base and near the top of the section give OSL ages 23.7 ± 5.5 and 17.5 ± 4.9 ka (Table 1, IS1 and IS2). These horizontally bedded post-Siwalik sediments on both limbs of the anticline represent growth strata deposited during the growth of the fold. These younger ages on the limbs of the growing JA corroborates the older timing of uplift of the anticline and growth of positive topography initiated at 42 ka.

Uplift, convergence and slip rates on the HFT

Prior to the rise of the JA ridge, alluvial fan sedimentation prevailed over the Panjab plain with fans originating from the Siwalik hinterland. The fan sediments were aggraded over the horizontally bedded foreland Siwalik. The JA was developed as a fault-propagation fold with pop-up style over the foreland advancing HFT (Powers et al. 1998). The post-Siwalik horizontal beds on both the limbs of the anticline show ~40° angular contact with the underlying tilted Siwalik, as observed at localities Ispur and Kothi. These were deposited during 24–12 ka as growth strata along with the erosion of the growing topography (Fig. 13b). The oldest OSL age 42.9 ± 3.5 ka of the fan sediments obtained from the hinge zone, immediately over the Siwalik, is assumed as the initiation time of the bed rock uplift and growth of the anticline in the central part. The central part, the interfluve's area of the AAF, was uplifted with lateral propagation of the JA (Malik et al. 2010a). The post-Siwalik fan cover sediments were largely eroded away from rest of the JAR, as revealed by the presence of interfluve remnants (Delcaillau et al. 2006). It is in the central segment of the JAR, which represents lateral propagation of the anticline fold, that the fan cover sediment remained preserved.

The JA in northwestern part is interpreted as a fault-propagation fold over the HFT with steeper, 45°SW, dipping forelimb and gentler, 30°NE, dipping backlimb (Powers et al. 1998). The backlimb is characterized by a blind back thrust, showing a pop-up geometry of the anticline. In southeastern part of the JA, adjoining our study area, near Bharatpur village southeast of Dejon, a fault scarp is observed (Malik et al. 2010b) facing southwest on the HFT trace. Recent trench investigation of the 15 m high measured fault scarp indicates a latest surface rupture with at least 9.3 m displacement that occurred between 1400 and 1460 AD (Kumahara and Jayangondaperumal 2013). The JA in southeastern part having a broad flat hinge zone suggests the existence and role of a back thrust in the formation of pop-up structure. As the HFT represents the surface expression of the MHT (decollement), the formation of JA

pop-up is ascribed due to shortening induced slip on the HFT-MHT and the back thrust-MHT.

The topographic uplift of the JA took place as a consequence of fault-propagation anticlinal growth resulting from slip on the HFT. The Siwalik strata with its cover of foreland fan sediments were folded into the JA. The average elevation of the Panjab plain near the mountain front is 350 m, and the average elevation of the uplifted plateau covered by the AAF is 500 m. This gives an elevation difference of 150 m. A similar value of 150 m uplift of the hinge zone culmination (plateau) from the Panjab plain is inferred by Delcaillau et al. (2006). This uplift represents the Siwalik bedrock uplift due to fold development. The abandoned alluvial fan (AAF) dated at 42.9 ± 3.6 ka has been uplifted 150 m relative to the Panjab plain. This gives an uplift (growth) rate of the anticlinal ridge at 3.4 ± 0.3 mm/year. The JA was developed as a fault-propagation pop-up fold over the HFT dipping 35°NE in the upper part and 25°NE in the lower part (mean 30º NE), inferred from seismic profile interpretation (Fig. 3b) (Powers et al. 1998). We have computed shortening rate based on 30°NE dip of the HFT, assuming that the HFT sole to the MHT with decreasing dip amount. Knowing the uplift rate and dip of the HFT, the convergence and slip rates calculated (Eqs. 3, 4; Supplementary Fig. S-d) on the HFT are 6.0 ± 0.5 and 6.9 ± 0.5 mm/year, respectively, over a period of 42.9 ± 3.5 ka. The slip rate is close to the estimated slip rate of 6.3 ± 2 mm/year on the HFT from a trench investigation at Mansa Devi near Chandigarh (Fig. 1), 80 km to the east of our locality (Malik and Nakata 2003). More recent paleoseismic study across the Hajipur fault scarps of the HFT near Beas River in northwestern termination of the JA gives late Holocene shortening rate of 6.9 ± 1.4 mm/year and slip rate of 7.6 ± 1.7 mm/year (Malik et al. 2010b). These estimated rates indicate that the Holocene shortening and slip rates on the HFT are closely similar to the long-term (late Quaternary) rates estimated in the present study. Using method similar to that applied for the HFT, the shortening and slip rates are calculated for the back thrust of the JA. The height (h') amsl difference between the anticline hinge zone strath surface and the Soan dun surface on the forelimb is 70 m, and dip of the back thrust fault is 40°. Using method described under methodology (Eqs. 3, 4), the shortening and slip rates are 2.0 ± 0.17 and 2.2 ± 0.18 mm/year, respectively. The estimated 6.0 mm/year shortening on the HFT and 2.0 mm/year shortening on the back thrust means that the HFT-back thrust (=MHT) has accommodated 8.0 mm/year shortening for the formation of JA.

Discussion

(a) The Kangra reentrant and the adjoining areas lie in the meizoseismal region of the 1905 Kangra earthquake of magnitude Mw 7.8. In the same area, a decade long instrumentally recorded seismicity indicates that the microseismicity is clustered north of the Kangra reentrant in the MBT–MCT zone and further north in the Chamba sequence of Lesser Himalaya, whereas the reentrant region south of the MBT is characterized by nearly absent to low microseismicity (Fig. 2) (Thakur et al. 2000; Kumar et al. 2009). The epicentral location of the 1905 Kangra earthquake is not well constrained, but it lies in the microseismicity zone north of the MBT. The southern extent of the 1905 Kangra earthquake rupture is inferred to lie on the JT based on geodetic measurements (Wallace et al. 2005). The southern extent of the instrumentally recorded microseismicity in the Kangra reentrant, which lies in the NW Himalaya, is clustered ~50 km north of the HFT. Whereas in the central Himalaya including Garhwal-Kumaun and Nepal, the southern extent of the microseismicity belt lies ~100 km north of the HFT (Arora et al. 2012; Jouanne et al. 2004). Microseismicity cluster is interpreted as a consequence of a deviatoric stress accumulation induced by transition between a locked part of the MHT and a northern part of the MHT affected by free, ductile creep beneath the topographic front of the Higher Himalaya. The strain accumulation occurs in the instrumental seismicity zone (Pandey et al. 1999; Bollinger et al. 2004) and is released periodically through slip by earthquakes that propagate southward and recorded as permanent displacement on the underlying decollement (Brun 1996; Bilham et al. 1998). The surface ruptures observed in the paleoseismology trenches inferring ≥250-km-long seismogenic faults on the Himalayan front (Lave et al. 2005; Kumar et al. 2006) are interpreted as the southward propagated earthquake ruptures. This interpretation is validated in the occurrence of surface rupture of great 1934 Bihar-Nepal earthquake, magnitude Mw 8.2, reported on the MFT at the Sub-Himalayan front (Sapkota et al. 2013). Likewise, the 2005 Kashmir earthquake, magnitude Mw 7.6, produced ~ 75 km surface rupture extending laterally and propagating ~50 km south of the epicenter and lying far north from the HFT in the hinterland (Kaneda et al. 2008; Hussain et al. 2009).

(b) GPS measurements in the central Nepal Himalaya indicate that a ~100-km-wide segment including the frontal part of the MHT between the Sub-Himalayan front and the southern extent of the instrumental seismicity zone is locked involving very little deformation, and 18–20 mm/year slip is consumed by ductile creep north of the Higher Himalaya where the MHT descends to greater depth (Bilham et al. 1997; Larson et al. 1999; Bettinelli et al. 2006). The GPS data show that the points located on the frontal Siwalik range anticlines are not affected by major motions during interseismic period which implies that the MHT is fully locked south of the locking line (Jouanne et al. 2004), and the major movement is largely coseismic along

the MHT that reach the ground surface south of the folds (Lave et al. 2005; Kumar et al. 2006; Jayangondaperumal et al. 2010). In the Kangra reentrant, the GPS measurements indicate that estimated 14 ± 1 mm/year shortening is accommodated at the southern edge of the Higher Himalaya, and there is little deformation across the ~100-km-wide zone south of the Higher Himalaya (Banerjee and Burgmann 2002). That implies that the position of the locking line is nearly the same in the reentrant of NW Himalaya as that in central Himalaya. However, its position with respect to the microseismicity belt has shifted toward the northern extent of the microseismicity cluster (Fig. 2).

(c) Using fluvial strath terraces, 21 ± 1.5 mm/year of Holocene N–S slip is estimated over the Main Frontal Thrust (MFT) in the central Himalaya, Nepal, suggesting that nearly the entire slip is consumed on the MFT (Lave and Avouac 2000). In the eastern Himalaya, Kameng of Arunachal Pradesh (AP) (Fig. 1), Holocene total shortening across 10-km-wide Main Himalayan Thrust (MHT) zone is estimated at 23.4 ± 6.2 mm/year. Here, the total shortening on the MHT zone is distributed across a wide zone, as ~8.4 mm/year on the Bhalukpong thrust, ~10 mm/year over the Ballipara anticline and ~5 mm/year on the Nimeri thrust (equivalent of MFT) (Burges et al. 2012). In the Kangra reentrant, our estimated long-term, late Quaternary, convergence rates on the HFT, the ST, and the JT are 6.0 mm/year over 42 ka, 3.0 mm/year over 29 ka, and 3.5–4.2 mm/year over 32–30 ka, respectively. These estimates suggest that the total shortening is distributed across a wide zone between the MBT and the HFT.

The geologically estimated shortening/slip rates decrease from central to northwest Himalaya and increases from central to eastern Himalaya along the Himalayan arc (Fig. 1a). It is 9–14 mm/year across the Potwar foreland structures in Pakistan (Baker et al. 1988), 1.4–4.1 mm/year along the Balakot-Bagh fault in Kashmir (Kaneda et al. 2008), 14 ± 2 mm/year across Kangra reentrant foreland structures (Powers et al. 1998) and 11.9 ± 3 mm/year on the HFT in Garhwal in NW Himalaya (Wesnousky et al. 1999) (Fig. 1a). The total Holocene shortening estimated in central Nepal is 21 ± 1.5 mm/year (Lave and Avouac 2000), and it is 23.4 ± 6.2 mm/year in Kameng of Arunachal Pradesh in the eastern Himalaya (Burges et al. 2012). The GPS-derived convergence rate of India with respect to Tibet increases from west to east (Bettinelli et al. 2006; Molnar and Stock 2009) (Fig. 1a). The current GPS-derived convergence is perpendicular to the Himalayan arc. The decreasing convergence rate from the central to the northwest Himalaya may be attributed to right-lateral slip in the NW Himalaya (Li and Yin 2008). The Kashmir Himalaya including the Kangra reentrant region, which lies close to the western Himalayan syntaxis showing a component of right-lateral slip, may imply oblique convergence (McCaffrey and Nabelek 1998; Jouanne et al. 1999).

(d) In the Kangra reentrant, the surface ruptures of historical earthquakes are reported on the HFT at Hajipur on the northwestern termination of the JA near Beas River (Malik et al. 2010a, b) and at Bharatpur showing 13 m slip in southeastern part of the JA (Kumahara and Jayangondaperumal 2013) (Fig. 1). These ruptures represent the great earthquakes with magnitude Mw > 8. The rupture of 1905 Kangra earthquake of magnitude <8 remained restricted to the hinterland (Wallace et al. 2005). The great earthquakes affect the flat of the MHT south of the locking line, whereas the 1905 Kangra and 2005 Kashmir-like earthquakes affect only a ramp above the MHT. (Pathier et al. 2006; Jouanne et al. 1999; Mugnier et al. 2013).

Conclusion

The Holocene long-term shortening rates are found to be consistent with the GPS-derived current ongoing shortening rates in Nepal and Garhwal Sub-Himalaya. This analogy can be extended temporally to include the late Quaternary shortening rates in the Kangra reentrant Sub-Himalaya. The Holocene total shortening accommodated on the MHT is recorded on the MFT (HFT) at the Himalayan front in the central sector of Himalaya, whereas the Holocene total shortening is distributed over a wide zone in Kameng (Arunachal) in the eastern Himalaya. This is analogous to partitioning of late Quaternary shortening rates in the Kangra reentrant of NW Himalaya. The geometry of the Siwalik foreland structures and simultaneous involvement of the entire package of Lower, Middle to Upper Siwaliks in the formation of fold-thrust system suggest that the foreland structures were formed during Quaternary time. The Sub-Himalaya includes a wide zone of active faults between the HFT and the MBT. The faults in the zone sole to the MHT. The total shortening is accommodated as a result of slip on the MHT. The thrust faults are reactivated by earthquakes originating in the ramp or flat of the MHT south of the Higher Himalaya. The earthquake surface rupture of the 1934 Bihar-Nepal earthquake has been observed on the MFT (HFT) at the Sub-Himalayan front, whereas the surface rupture of 2005 Kashmir earthquake has been mapped in the hinterland of Sub-Himalaya. Historical seismology data reveal that there are two categories of earthquakes in the Himalaya: the great to mega thrust earthquakes with magnitude Mw > 8 and the large earthquakes with magnitude Mw < 8, between 7 and 8. It appears that the larger ruptures, >100 km wide, of the great earthquakes, e.g., 1934 Bihar-Nepal, emerge at the Himalayan front reactivating the HFT. The smaller ruptures, <100 km, of the large earthquakes, like the large 2005 Kashmir and 1905 Kangra,

reactivated the preexisting faults and remained restricted to the hinterland. This may imply that the large earthquakes originated along the MHT ramp reactivating the faults; whereas the great earthquakes occurred along the locked part of the MHT flat from the locking line to the surface. In large earthquakes, the slip may be transferred from the MHT to the preexisting hinterland faults, for example MHT- JT segment in case of 1905 Kangra earthquake and MHT-Balakot Fault in 2005 Kashmir earthquake. In great to mega earthquakes, having wider rupture, the slip is propagated to the MHT-HFT segment at the Himalayan front.

Acknowledgments The study was funded by the Seismology Division of the Department of Science and Technology, now Ministry of Earth Sciences. We are grateful to the Director, WIHG, for providing the logistic of OSL laboratory facility and administrative support. We thank F. Jouanne, F. Audemard, S. Mukherjee and an anonymous reviewer for their comments.

References

Ambreys N, Bilham R (2000) A note on the Kangra Ms = 7.8 earthquake of 4 April 1905. Curr Sci 79:101–106

Armijo R, Tapponnier P, Mercier JL, Tonglin H (1986) Quaternary extension in southern Tibet. J Geophys Res 91:13803–13872

Arora BR, Gahlaut VK, Kumar N (2012) Structural control on along strike variation in the seismicity of northwest Himalaya. J Asian Earth Sci 57:15–24

Avouac JP, Tapponnier P (1993) Kinematic model of active deformation in central Asia. Geophys Res Lett 20:895–898

Baker DM, Lillie RJ, Yeats RS, Johnson GD, Yousuf M, Zamin AH (1988) Development of the Himalayan frontal thrust zone: salt range, Pakistan. Geology 16:3–7

Banerjee P, Burgmann R (2002) Convergence across the northwest Himalaya from GPS measurements. Geophys Res Lett 29:30-1–30-4

Bettinelli P, Avouac JP, Flouzat M, Jouanne F, Bollinger L, Willis P, Chitrakar GJ (2006) Plate motion of India and interseismic strain in Nepal Himalaya from GPS and DORIS measurements. J Geod. doi:10.1007/s00190-006-003-3

Bilham R, Larson K, Freymuller J (1997) Indo-Asian convergence rates in Nepal Himalaya. Nature 386:61–66

Bilham R, Blum F, Bendick R, Gaur VK (1998) Geodetic constraints on the translation and deformation of India, implications for future great Himalayan earthquakes. Curr Sci 74:213–219

Bollinger L, Avouac JP, Cattin R, Pandey MR (2004) Stress building in the Himalaya. J Geophys Res 109, BIP 405:1–8

Brun JN (1996) Particle motions in a physical model of shallow angle thrust faulting. Proc Indian Acad Sci Earth Planet Sci 105:197–206

Burbank DW, Anderson RS (2011) Tectonic geomorphology. Wiley, Oxford, p 454

Burbank DW, Leland J, Fielding E, Anderson RS, Brozovic N, Reid MR, Duncan C (1996) Bedrock incision, rock uplift and threshold hill slopes in the northwestern Himalaya. Nature 379:505–510

Burges WP, Yin A, Dubey CS, Shen ZK, Kelty TK (2012) Holocene shortening across the Main Frontal Thrust zone in the eastern Himalaya. Earth Planet Sci Lett 357–358:152–167

Delcaillau B, Carozza JM, Laville E (2006) Recent fold growth and drainage development: the Janauri and Chandigarh anticlines in the Siwalik foothills, northwest India. Geomorphology 76:241–256

Dutta S, Suresh N, Kumar R (2012) Climatically controlled Late Quaternary terrace staircase development in the fold and—thrust belt of Sub-Himalaya. Paleogeog Paleoclimat Paleoecol 356:16–26

Hussain A, Yeats RS, Mona Lisa (2009) Geological setting of the 8th October, 2005 Kashmir earthquake. J Seism 13:315–325. doi:10.1007/s/10950-800-9101-7

Jayangondaperumal R, Dubey AK, Kumar BS, Wesnousky SG, Sangode SJ (2010) Magnetic fabrics indicating Late Quaternary seismicity in the Himalayan foothills. Int J Earth Sci (Geol Rundschau) 99(Suppl 1):S265–S278. doi:10.1007/00531-009-0494-5

Jayangondaperumal R, Mugnier JL, Dubey AK (2013) Earthquake slip estimation from the scarp geometry of Himalayan Frontal Thrust, western Himalaya: implications for seismic hazard assessment. Int J Earth Sci (Geol Rundschau) 102:1937–1955. doi:10.1007/s00531-013-0888-2

Jouanne F, Mugnier JL, Pandey MR, Gamond JF, LeFort P, Serrurier L (1999) Oblique convergence in the Himalayas of western Nepal deduced from preliminary results of GPS measurements. Geophys Res Lett 26:1933–1936

Jouanne F, Mugnier JL, Gamond JF, LeFort P, Pandey MR, Bollinger L, Flouzat M, Avouac JP (2004) Current shortening across the Himalayas of Nepal. Geophys J Int 157:1–14

Kaneda H, Nakata T, Tsumi H, Kando H et al (2008) Surface rupture of the 2005 Kashmir, Pakistan, earthquake and its active tectonics. Bull Seism Soc Am 98:521–557

Karunakaran C, Rao R (1979) Status of hydrocarbon in the Himalayan region : Contributions to stratigraphy and structure. Geol Surv India. Miscellaneous Publication 41:1–66

Kumahara Y, Jayangondaperumal R (2013) Paleoseismic evidence of a surface rupture along the northwestern Himalayan Frontal Thrust. Geomorphology 180–181:47–56

Kumar S, Wesnousky SG, Rockwall TK, Briggs RW, Thakur VC, Jayangondaperumal R (2006) Paleoseismic evidence of great surface rupture earthquake along the Indian Himalaya. J Geophys Res III, Bo3304. doi:10.1029/2004JB00309

Kumar N, Sharma J, Arora BR, Mukhopadhyay S (2009) Seismotectonic model of the Kangra-Chamba sector of Northwest Himalaya: constraints from joint hypocenter determination and focal mechanism. Bull Seism Soc Am 99:95–109

Larson K, Bergmann R, Bilham R, Freymueller JT (1999) Kinematics of the India-Eurasian collision zone from GPS measurements. J Geophys Res 104:1077–1093

Lave J, Avouac JP (2000) Active folding of fluvial terraces across the Siwalik Hills, Himalayas of Central Nepal. J Geophys Res 105:5735–5770, 593. doi:10.1029/1999JB900292

Lave J, Avouac JP (2001) Fluvial incision and tectonic uplift across the Himalayas of Central Nepal. J Geophys Res 106:26561–26591. doi:10.1029/2001JB000359

Lave J, Yule D, Sapkota S, Basant K, Madden C, Attal M, Pandey MR (2005) Evidence of a great Medieval earthquake (~1100AD) in the Central Nepal. Science 307:1302–1305

LeFort P (1975) Himalayas collided range-present knowledge of continental arc. Am J Sci A275:1–44

Li DW, Yin A (2008) Orogen-parallel, active left-slip faults in the Eastern Himalaya: implications for the growth mechanism of the Himalayan arc. Earth Planet Sci Lett 274:258–267

Lyon-Caen H, Molnar P (1985) Gravity anomalies, flexure of Indian plate and the structure, support, and evolution of the Himalayan Ganga basin. Tectonics 4:513–538

Malik JN, Mohanty C (2006) Active tectonics influence on the evolution of drainage and landscape: geomorphic signatures from frontal and hinterland areas along the Northwestern Himalaya, India. J Asian Earth Sci 12:489–518

Malik JN, Nakata T (2003) Active faults and related Late Quaternary deformation along the Northwestern Himalayan Frontal Zone, India. Annal Geophys 46(5):917–936

Malik JN, Shah AA, Sahoo AK, Puhan B, Banerjee C, Shinde DP, Juyal N, Singhvi AK, Rath S (2010a) Active fault, fault growth and segment linkage along the Janauri anticline (fontal foreland fold), NW Himalaya, India. Tectonophysics 483:327–343

Malik JN, Sahoo AK, Shah AA, Shinde DP, Juyal N, Singhvi AK (2010b) Paleoseismic evidence from trench investigation along Hajipur fault, Himalayan Frontal Thrust, NW Himalaya. Implication of faulting pattern on landscape evolution and seismic hazard. J Tructural Geol 32:350–361

McCaffrey R, Nabelek J (1998) Role of oblique convergence in the Himalayas and southern Tibet plateau. Geology 26:691–694

Medlicott HB (1864) On the geological structure and relations of the southern portion of the Himalayan ranges between rivers Ganges and the Ravi. Mem Geol Surv Ind 3(2):1–122

Middlemiss CS (1910) Kangra earthquake of 4th April, 1905. Mem Geol Surv India 39:1–409

Molnar P (1984) Structure and tectonics of the Himalaya: constraints and implication of geophysical data. Ann Rev Earth Planet Sci 12:489–518

Molnar P, Stock JM (2009) Slowing of India's convergence with Eurasia since 20 Ma and its implications for Tibetan mantle dynamics. Tectonics 28:TC3001. doi:10.1029/2008TC00227

Mugnier JL, Gajure A, Huyghe P, Jayangndaperumal R, Jouanne F, Upreti BN (2013) Structural interpretation of the great earthquakes of the last millennium in the central Himalaya. Earth Sci Rev 127:30–47

Mukherjee S (2013) Channel flow extrusion model to constraint dynamic viscosity and Prandtl number of the Higher Himalayan Shear Zone. Int J Earth Sci 102:1811–1835

Mukherjee S (2014) A review on out-of-sequence deformation in the Himalaya. In: Mukherjee S, Carosi R, Mukherjee BK, Robinson D, Vander der Beek P (eds) Geol Soc Lond. Spec Vol (in press)

Mukherjee S, Koyi HA, Talbot C (2012) Implications for channel flow analogue models for extrusion of the Higher Himalayan Shear Zone with special reference to out-of–sequence thrusting. Int J Earth Sci 101:253–273

Mukul M, Jaiswal M, Singhvi AK (2007) Timing of recent out of sequence active deformation in the frontal Himalayan wedge: insights from Darjeeling Sub-Himalaya. Geology 35:999–1002

Murray AS, Wintle AG (2000) Luminescence dating of quartz using an improved single-aliquot regenerative dose protocol. Radiat Meas 32:57–73

Nabelek J, HI-CLIMB Team (2009) Underplating in the Himalaya-Tibet collision zone revealed by the Hi-CLIMB experiment. Science 325(5946):1371–1374. doi:10.1126/1167719

Ori G, Friend PF (1984) Sedimentary basins formed and carried back on a active thrust sheets. Geology 12:475–476

Owen LA, Bailey RM, Rhodes EJ, Mitchell WA, Coxon P (1997) Style and timing of glaciation in the Lahul Himalaya, northern India: a framework for reconstructing late Quaternary palaeoclimatic change in the western Himalayas. J Quat Sci 12:83–109

Owen LA, Finkel RC, Caffee MW (2002) A note on the extent of glaciation in the Himalaya during the global Last Glacial Maximum. Quat Sci Rev 21:147–158

Pandey MR, Tandulkar RP, Avouac JP, Vergne J, Heritier TH (1999) Seismotectonics of the Nepal Himalaya from a local seismic network. J Asian Earth Sci 17:703–712

Pathier E, Fielding EJ, Wright TJ, Walker R, Parsons BE, Hensley S (2006) Displacement field and slip distribution of the 2005 Kashmir earthquake from SAR imagery. Geophys Res Lett 33:L20310. doi:10.1029/2006GL027193

Peltzer G, Saucier F (1996) Present day kinematics of Asia derived from geological fault rates. J Geophys Res 101:27943–27956

Powers PM, Lillie RJ, Yeats RS (1998) Structure and shortening of the Kangra and Dehradun re-entrants, Sub-Himalaya, India. Geol Soc Am Bull 110:1010–1027

Raiverman V, Srivastava AK, Prasad DN (1994) Structural style in northwestern Himalayan foothills. Himal Geol 15:263–280

Rockwell TK, Keller EA, Clak MN, Johnson DL (1984) Chronology and rates of faulting of Ventura river terraces, California. Geol Soc Am Bull 95:1466–1476

Sapkota SN, Bollinger L, Klinger L, Tapponnier P, Gaudemer Y, Tewari D (2013) Primary surface ruptures of the great Himalayan earthquakes in 1934 and 1255. Nat Geosci 6:71–76

Schulte-Pelkum V, Monslav G, Sheehan A, Pandey MR, Bilham R, Wu F (2005) Imaging the Indian subcontinent beneath the Himalaya. Nature 435:1223–1225

Srivastava P, Rajak MK, Singh LP (2009) Late Quaternary alluvial fans and paleosols of the Kangra basin, NW Himalaya: tectonic and paleoclimatic implication. Catena 76:135–154

Suppe J (1983) Geometry and kinematics of fault-bend folding. Am J Sci 283:659–672

Suresh N, Kumar R (2009) Variable period of aggradations and termination history of two distinct late Quaternary fans in the Soan Dun, NW Sub-Himalaya: impact of tectonics and climate. Himal Geol 30:155–166

Thakur VC (1998) Structure of Chamba nappe and position of the main Central Thrust in Kashmir Himalaya. J Asian Earth Sci 16:269–282

Thakur VC (2013) Active tectonics of Himalayan Frontal Fault system. Int J Earth Sci (Geol Rundsch). doi:10.1007/00531-013-0891-7

Thakur VC, Sriram V, Mundepi AK (2000) Seismotectonics of great 1905 Kangra earthquake meizoseismal region in Kangra-Chamba, NW Himalaya. Tectonophysics 32:289–298

Thakur VC, Pandey AK, Suresh N (2007) Late Quaternary-Holocene frontal fault zone of the Garhwal Sub Himalaya, NW India. J Asian Earth Sci 29(2/3):305–319

Thakur VC, Jayangondaperumal R, Malik MA (2010) Redefining Wadia-Medlicott's Main Boundary Fault from Jhelum to Yamuna: an active fault strand of the Main Boundary Thrust in Northwest Himalaya. Tectonophysics 489:29–42

Wadia DN (1937) PermoCarboniferous limestone inliers in the Sub-Himalayan Tertiary zone of Jammu, Kashmir Himalaya. Rec Geol Surv Ind 72:162–173

Wallace K, Bilham R, Blum F, Gaur VK, Gahlaut V (2005) Surface deformation in the region of the 1905 Kangra Mw = 7.8 earthquake in the period 1846-2001. Geophys Res Lett 32:L 15307. doi:10.1029/2005GL022906

Wesnousky SG, Kumar S, Mahindra R, Thakur VC (1999) Uplift and convergence along the Himalayan Frontal Thrust of India. Tectonics 18:967–976

Wobus CW, Whipple KX, Hodges KV (2006) Neotectonics of the Central Nepalese Himalaya: constraints from geomorphology, detrital $^{40}Ar/^{39}Ar$ thermochronology and thermal modeling. Tectonics 25. TC 4011. doi:10.1029/2005TC001935

Yeats RS, Nakata T, Farah A, Mirza MA, Pandey MR, Stein RS (1992) The Himalayan Frontal Fault System. In: Bucknam RC, Hancock PL (eds) Major active faults of the world: results of IGCP project 206: Annales Tectonicae, Supp To V. V I, pp 85–98

Yin A (2006) Cenozoic tectonic evolution of the Himalayan orogen as constrained by along-strike variation of structural geometry, exhumation history, and foreland sedimentation. Earth Sci Rev 28:211–280

Zhou W, Nelson KD, Project INDEPTH team (1993) Deep seismic reflection evidence for continental underthrusting beneath southern Tibet. Nature 302:557–559